國 立 交 通 大 學

電信工程研究所

碩 士 論 文

無線隨意網路中針對接收端阻隔問題提出適應性收端傳送協定之設計與分析

Design and Analysis of Adaptive Receiver Transmission Protocols for Receiver Blocking Problem in Wireless Ad-Hoc Networks

研 究 生：雷惟能

指導教授：方凱田 教授

中 華 民 國 壹 百 年 三 月

無線隨意網路中針對接收端阻隔問題提出適應性收端傳送協定之設計與分析

Design and Analysis of Adaptive Receiver Transmission Protocols for Receiver Blocking Problem in Wireless Ad-Hoc Networks

研 究 生：雷惟能　　　　　Student：Wei-Neng Lei

指導教授：方凱田　　　　　Advisor：Kai-Ten Feng

國 立 交 通 大 學

電信工程研究所

碩 士 論 文

A Thesis
Submitted to Institute of Communications Engineering
College of Electrical and Computer Engineering
National Chiao Tung University
in Partial Fulfillment of the Requirements
for the Degree of
Master of Science
in

Communications Engineering

March 2011

Hsinchu, Taiwan, Republic of China

中華民國壹百年三月

無線隨意網路中針對接收端阻隔問題提出適應性收端傳送協定之設計與分析

學生：雷惟能　　　　　　　　　　　　　指導教授：方凱田

國立交通大學電信工程研究所碩士班

摘　　　要

　　分散式的無線網路環境中，因缺乏統籌管理無線資源的協調者，因此媒體存取控制(MAC)協定之設計會是重要的議題。無線隨意網路在吞吐量上的效能表現不彰，尤其接收端阻隔問題更進一步惡化無線隨意網路的效能，因此本論文提出多重收端傳送機制(MRT)以及快速網路配置向量截斷機制(FNT)來減緩接收端阻隔問題而不必額外再採用控制通道以及傳輸天線。為了進一步提升 MRT 以及 FNT 之系統效能，本論文尚提出適應性收端傳送協定(ART)，以及可支援動態收端數目調整之演算法(ART-DA)。爾後，本研究針對 ART 通訊協定建立數學模型分析其效能，透過電腦模擬亦驗證了分析結果的準確性。此外，模擬結果同時也與已存在對抗接收端阻隔問題的通訊協定進行比較，顯示本研究提出的通訊協定以及搭配的演算法能更有效率的解決接收端阻隔問題，提升整體無線隨意網路的系統吞吐量。

Design and Analysis of Adaptive Receiver Transmission Protocols for Receiver Blocking Problem in Wireless Ad-Hoc Networks

Student : Wei-Neng Lei   Advisor : Kai-Ten Feng

Institute of Communications Engineering
National Chiao Tung University

Abstract

Due to the lack of a centralized coordinator for wireless resource allocation, the design of medium access control (MAC) protocols is considered crucial for throughput enhancement in the wireless ad-hoc networks. The receiver blocking problem, which has not been studied in most of the MAC protocol design, can lead to severe degradation on the throughput performance. In this thesis, the multiple receiver transmission (MRT) and the fast NAV truncation (FNT) mechanisms are proposed to alleviate the receiver blocking problem without the adoption of additional control channels. The adaptive receiver transmission (ART) scheme is proposed to further enhance the system throughput with dynamic adjustment of the selected receivers. Analytical model is also derived to validate the effectiveness of the proposed ART protocol. Simulations are performed to evaluate and compare the proposed three protocols with existing MAC schemes. It can be observed that the proposed ART protocol outperforms the other schemes by both alleviating the receiver blocking problem and enhancing the system throughput for the wireless multi-hop ad-hoc networks.

Contents

List of Figures

Chapter 1

Introduction

A wireless multi-hop network (WMN) [1] adopts wireless communication technologies to maintain connectivity and exchange messages between decentralized nodes in the multi-hop manners. This type of wireless networks are capable to perform self-creating, administering, and organizing the network connectivity. With the decentralized characteristics of the WMNs, feasible design of medium access control (MAC) protocol is considered important for performance enhancement. However, the connectivity between the network nodes are in general not guaranteed in the WMN, which incurs notorious exposed node and hidden node problems [2]. Some early attempts for resolving these problems in the literature [3–6] suggested the usage of request-to-send (RTS) and clear-to-send (CTS) mechanisms, which were later adopted by the IEEE 802.11 standards. The well-adopted IEEE 802.11 MAC protocol suite [7–10] can be employed in the WMNs since it has been specified to support decentralized operations called the ad-hoc mode.

However, it has been studied [11,12] that the deployment of ad-hoc mode in the IEEE 802.11 network does not always result in feasible performance. Even though the hidden node and exposed node problems can be partially

alleviated by adopting the distributed coordination function (DCF) in the IEEE 802.11-based protocols, an extended problem called receiver blocking or unreachability will be induced by the hidden node and exposed node problems thereafter. The receiver blocking problem occurs when the intended destination is located within the coverage of an on-going transmission pair. The destination node is not able to response to the corresponding RTS packet from the sender since the destination will be in the silent state caused by either the virtual carrier sensing (VCS) or the physical carrier sensing (PCS). In such case, the source node which is outside the range of this on-going transmission pair will confront a series of connection failure with its destination, which will result in the increase of unnecessary control overheads by initiating the RTS packets. The receiver blocking problem, which has not been addressed in the IEEE 802.11 standards, should deserve attention from research work since it will cause severe degradation on network throughput. The formal definition of the receiver blocking problem will be described in Chapter 3.

It has been investigated in several studies [13–20] regarding the severe performance degradation in ad-hoc networks. The dual-channel (DUCHA) [15] MAC protocol was proposed to alleviate the receiver blocking problem by adopting an additional channel for the transmission of control packets; while the data packet is transmitted in the data channel. The busy tone (BT) is adopted in the DUCHA protocol for the delivery of data packet; while the other nodes that hear the BT should suspend their attempts for data transmissions. The half-restraint carrier sense scheme (HCSS) [16] suggested a reduced carrier sensing threshold for receiver blocking avoidance. However, smaller carrier sensing threshold, which results in less spatial reuse, can significantly cause the reduction of network throughput. Ye et al. [17] proposed a jamming-based MAC (JMAC) protocol to remove the hidden ter-

minal problem since each node will be equipped with two transceivers which independently operate in two separate channels, called the S-channel and the R-channel. As the destination is receiving the data packet on the S-channel, the other transceiver in the destination will broadcast the jamming signal on the R-channel which is considered a pseudo-noise in order to trigger the PCS mechanism from the heard neighbors. The channel will be marked as in the busy state such that the destination will not be interfered by its neighbors for the reception of data packets. However, each network node is required to install at least two transceivers in [15, 17] which is not always considered realistic due to hardware limitation and cost. In addition to the increase of hardware cost, the limited battery capacity in most mobile devices will constrain the adoption of multiple transceivers on each node since either the busy tone or the jamming signal can result in considerable energy consumption. Moreover, with the installation of multiple transceivers, the BT-based and JMAC schemes will not sufficiently utilize the advantages of spatial dimension which can cause poor multiplexing gain or diversity gain in a multiple-input multiple-output (MIMO) system [21]. The major reason is that the second transceiver is merely utilized for the transmission of either the busy tone or the jamming signal.

In this thesis, the multiple receiver transmission (MRT) and the fast NAV truncation (FNT) mechanisms are proposed to cope with the receiver blocking problem without adopting either additional control channels or transceivers. The MRT approach is proposed to provide additional opportunities for the transmission to multiple receivers; while the FNT scheme reduces the duration of the network allocation vector (NAV) in order to provide channel accessing opportunities for the other nodes in the network. However, both the MRT and FNT schemes may suffer performance degradation under specific network scenarios which lead to the proposal of adaptive

receiver transmission (ART) protocol in order to further enhance the network efficiency and channel utilization. The analytical model for throughput performance of the proposed ART protocol will be derived and further validated with simulations. The performance evaluation of the proposed schemes will be performed and compared with the conventional IEEE 802.11a DCF protocol and other existing schemes via simulations. It will be shown that the receiver blocking problem can be effectively alleviated with the adoption of proposed MRT, FNT, and ART schemes. The network throughput can consequently be enhanced.

The rest of this thesis is organized as follows. In Chapter 2, a summary of related works is given. Chapter 3 describes the network model and the receiver blocking problem. The proposed MRT, FNT, and ART mechanisms are explained in Chapter 4; while the throughput analysis for ART protocol is derived in Chapter 5. Performance evaluation of these three schemes is shown in Chapter 6. Chapter 7 draws the conclusions.
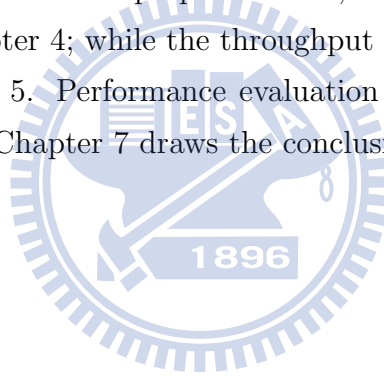
Chapter 2

Related Work

The DUCHA protocol proposed in [15] is one of the earliest literature approaching the receiver blocking problem which is inspired from the dual busy-tone multiple access (DBTMA) scheme. Haas et al. [22–24] presented the DBTMA mechanism that utilized two out-of-band busy tones, including BT_t transmitted by the source node to inform all nodes within its transmission range and BT_r delivered by the destination node to notify all the nodes within the destination's coverage. If a node overhears the busy tone signal, it must be kept in the silent state in order to avoid possible collision. Even thought this approach can well-address the hidden terminal problem, it is required to provide both an additional channel and an additional transceiver for implementation. Several schemes have been proposed in [25–27] for performance enhancement based on the DBTMA protocol. In [25, 26], without significant loss on throughput performance, the authors utilized only one busy tone channel to implement all the functionalities required by the DBTMA approach. The protocol proposed in [27] further improved the throughput performance by enlarging the carrier sensing range of the transmitter's busy-tone channel.

Zhai and Fang [28] proposed a new MAC protocol, called short busy advertisements MAC (SBA-MAC), in which the sender inserts a few dummy bits in one data frame. During the time of dummy bits, the intended receiver transmits the short busy advertisements (SBA) over the same channel to clear the channel for data reception. The receiver will continue the reception of its remaining data packets afterwards. Therefore, it is only required for each node to equip one transceiver and the protocol can be operated in a single channel. However, the severe RTS packet collisions still remain unresolved which is considered the major challenge for ad-hoc networks. On the other hand, the eMAC protocol [29] is proposed based on a multiple access collision avoidance (AMACA) protocol [30] to deal with the receiver blocking problem. The eMAC-table contains partial topology information of a network node and is periodically exchanged between the neighbor nodes. Therefore, a node can maintain and utilize the dual-hop neighborhood graph to determine the best strategy for the transmission of individual communication pause (ICP) packet which solves the ICP broadcast storm problem in the original AMACA protocol. Note that the ICP packet is utilized when a network node is notified to be silent for a NAV duration and unfortunately becomes unreachable. Those unreachable nodes are provided with the opportunities to inform their one-hop neighbors about the upcoming unreachability by using the ICP packets, which are broadcast after the RTS/CTS negotiation and before the data transmission. Consequently, a network node will not establish the connection with those unreachable nodes after successfully receiving the ICP packets. Similar concepts are also adopted in [31].

Moreover, a enhanced IEEE 802.11 protocol that operates similar to the conventional DCF scheme is proposed in [32], which is called eDCF protocol in this thesis for notation convenience. After sending the RTS packet to the intended receiver, the source node will set a timeout duration wait-

6

ing for the CTS response. If the CTS packet has not been received after the timeout period, the eDCF scheme will provide an additional opportunity to select another receiver from its queue to deliver data packet since this channel within the coverage of the source node has already been reserved. Therefore, the RTS packet is not wasted even the channel is erroneously reserved, and the source node will not repeatedly construct the connection to a blocked receiver. On the other hand, Jiang and Liew claimed that the proposed schemes in [33] are the first attempt for a comprehensive and rigorous study on both the hidden node and exposed node problems. This work indicates that these two problems are generally a tradeoff, which are considered difficult to be entirely removed in the network. The authors expressed the exposed node and hidden node problems based on several constraints, and these two problems can be removed if the designed constraints are not satisfied. The selective disregard of NAVs (SDN) scheme is proposed to break the constraints for the exposed node problem. The concept of SDN scheme is to turn off the PCS mechanism and the transmission is allowed only depending on the NAV period regardless of whether the medium is physically sensed busy or idle, which consequently resolves the exposed terminal problem. However, the deactivation of PCS mechanism may potentially cause hidden node problem. Therefore, the hidden-node free design (HFD), inherited from [34], is proposed to compensate the drawbacks of SDN scheme by enlarging the range of PCS mechanism. However, the HFD scheme should operate with "restart mode" which is not utilized by default in most of the commercial IEEE 802.11 chips. The details about the "restart mode" can be referred in [34].

Furthermore, the work in [35] balanced the hidden node and exposed node problems by providing adequate power control to appropriately adjust the transmission, carrier sensing, and interference ranges. The approaches pro-

posed in [36–42] provide another category to alleviate the receiver blocking, the hidden node, and the exposed node problems by separating the traffic loads on multiple channels. However, the multichannel hidden terminal problem will be induced which can be a more complicate problem within the multichannel architecture. Finally, mathematical models on throughput analysis have been presented in [43–49] for contention-based channel access systems. These models will be referred in the performance analysis of proposed ART protocol, which will be described in Chapter 5.
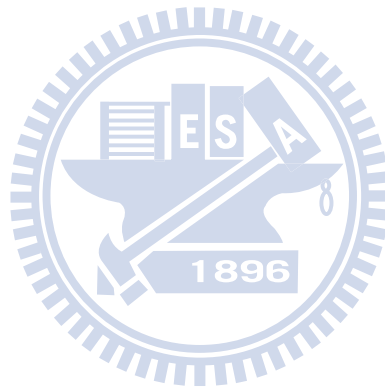
Chapter 3

Network Model and Problem Statement

Considering a set of nodes $\mathbf{N} = \{N_i \,|\, \forall\, i\}$ within a two-dimensional Euclidean plane, the locations of the set $\mathbf{N}$ are represented by the set $\mathbf{P} = \{P_{N_i} \,|\, P_{N_i} = (x_{N_i}, y_{N_i}), \forall i\}$. It is assumed that all the nodes are homogeneous and equipped with omnidirectional antennas under a single channel. The set of closed disks defining the transmission ranges of $\mathbf{N}$ is denoted as $\overline{\mathbf{D}} = \{\overline{D}(P_{N_i}, R) \,|\, \forall\, i\}$, where $\overline{D}(P_{N_i}, R) = \{x \,|\, \|x - P_{N_i}\| \leq R, \forall\, x \in \mathbb{R}^2\}$. It is noted that P_{N_i} is the center of the closed disk with R denoted as the radius of the transmission range for each N_i. Each node in the transmission range $\overline{D}(P_{N_i}, R)$ can communicate with N_i by utilizing the IEEE 802.11-based MAC features for channel allocations, including PCS, VCS, and binary exponential backoff (BEB) [50]. Moreover, the one-hop neighbor table for each N_i is defined as $\mathbf{T}_{N_i} = \{N_k \,|\, P_{N_k} \in \overline{D}(P_{N_i}, R), \forall\, k \neq i\}$. The receiver blocking problem associated with the receiver blocking group are defined as follows.

Definition 1 (Receiver Blocking Group). Given the set $\mathbf{S} \subseteq \mathbf{N}$ which
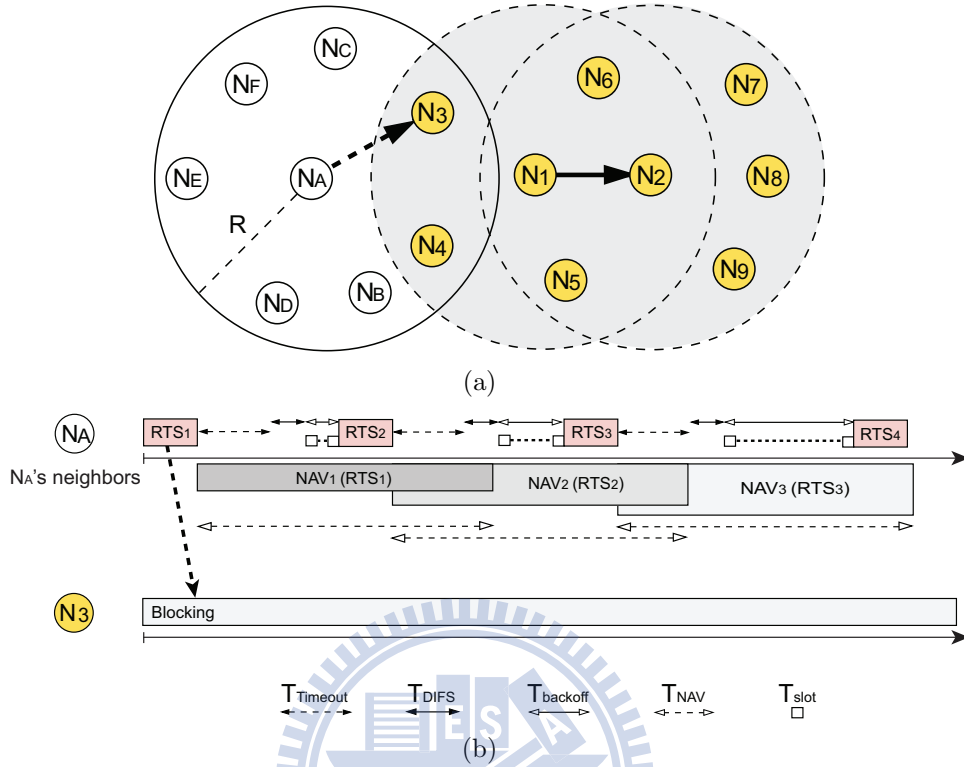
Figure 3.1: The schematic diagram for the receiver blocking problem: (a) the network topology; (b) the timing diagrams of N_A and N_A's neighbors.

includes all the transmitters and receivers, the receiver blocking group is defined as $\mathbf{B} = \bigcup_{N_i \in \mathbf{S}} \mathbf{T}_{N_i}$ since all the nodes in $\mathbf{B}$ are blocked either by the carrier sensing mechanisms or due to the on-going packet transmission.

Problem 1 (Receiver Blocking Problem). Let $\mathbf{B}$ be the receiver blocking group within the network. The receiver blocking problem occurs while a node $N_i \in (\mathbf{N} - \mathbf{B})$ intends to communicate with a node $N_j \in \mathbf{B}$. Due to the blocking nature of N_j, a large amount of useless connection-request packets will be issued by N_i, which leads to the degradation of network throughput.

Fig. 3.1 illustrates the schematic diagram for the receiver blocking problem with the network topology and the corresponding timing diagram. As

shown in Fig. 3.1(a), it is considered that N_1 and N_2 constitute the on-going transmission pair as identified by the solid arrow. The receiver blocking problem happens if $N_A \in (\mathbf{N} - \mathbf{B})$ intends to initiate a communication link with $N_3 \in \mathbf{B}$, i.e. denoted by the dashed arrow. Based on Definition 1, the receiver blocking group is obtained as $\mathbf{B} = \{N_1, ..., N_9\}$, which lies within the light gray region as in Fig. 3.1(a). Referring to Fig. 3.1(b), N_A will attempt to communicate with N_3 by transmitting the RTS packet (i.e. RTS$_1$) after the successful channel contention. Based on the broadcast nature, N_B and N_C will also receive the RTS$_1$ packet and consequently set up their corresponding NAV timers in order to refrain from accessing the channel, i.e. $T_{NAV} = T_{CTS} + T_{Data} + T_{ACK} + 3T_{SIFS} + 3T_{prop}$. It is noted that the subscript in each timing parameter is utilized to denote its corresponding meaning, i.e. T_{CTS}, T_{Data}, T_{ACK}, T_{SIFS}, and T_{prop} indicate the time durations for the CTS packet, data packet, ACK packet, the short inter-frame space, and the propagation delay respectively. Moreover, T_{slot} and T_{DIFS} in Fig. 3.1(b) represent the slot time of conventional IEEE 802.11 standard and the time duration for the DCF inter-frame space respectively; while the parameter $T_{backoff}$ indicates the time interval for the current backoff window of a node.

However, N_3 will not respond to the RTS$_1$ packet with a corresponding CTS packet due to the PCS/VCS mechanisms. After a timeout $T_{timeout} = T_{CTS} + T_{SIFS} + T_{prop}$ for waiting the CTS packet, N_A will double its backoff window and re-initiate to communicate with N_3 by sending another RTS packet, i.e. the RTS$_2$ packet. In the meantime, N_B and N_C will refresh their corresponding NAV timers based on the newly issued RTS$_2$ packet as in Fig. 3.1(b). Consequently, N_A will result in a great amount of useless retries of sending RTS packets, which prohibit N_B and N_C from contending the channel and lead to the degradation of network throughput.

Chapter 4

Proposed MAC Protocols

For the purpose of alleviating the receiver blocking problem and its resulting drawbacks, three MAC schemes are proposed in this chapter, i.e. the multiple receiver transmission (MRT), the fast NAV truncation (FNT), and the adaptive receiver transmission (ART) protocols. Note that the FNT scheme can be jointly implemented with the MRT mechanism in order to further enhance the network throughput.

4.1 Multiple Receiver Transmission (MRT) Scheme

According to Definition 1, all nodes in the receiver blocking group $\mathbf{B}$ will not respond to the node $N_i \in (\mathbf{N} - \mathbf{B})$. Therefore, the transmission of the RTS packets from N_i will fail in constructing the communication links to the nodes in $\mathbf{B}$. It is noticed that the unsuccessful reception of the CTS packets by N_i can be attributed to the factors as follows: (a) packet collisions; (b) error reception of the CTS packet from the receiver; and (c) the receiver locating in the receiver blocking group $\mathbf{B}$. If the failure of acquiring the CTS

packets is due to the factors (a) and (b), the conventional BEB method can be adopted to effectively resolve the drawbacks of the missing CTS packets by expanding the contention window and retransmitting the RTS packets. However, the BEB scheme will not suffice for alleviating factor (c), which will in general result in excessive and ineffective transmissions of the RTS packets.

One intuitive method to resolve factor (c) is to terminate the retransmission of the RTS packets since the RTS retries have no contribution in constructing the communication links with the node in $\mathbf{B}$ [29]. However, it requires node N_i to possess the information that the receiver is located within $\mathbf{B}$, which is considered inapplicable in realistic cases. The design concept of the proposed MRT technique is to increase the probability for selecting the destination that does not belong to the receiver blocking group $\mathbf{B}$. Instead of merely transmitting the RTS packet to its original intended receiver in $\mathbf{B}$, N_i will also attempt to utilize the same RTS packet for constructing the communication links with the other receivers which are not in the set $\mathbf{B}$, e.g. N_C as in Fig. 3.1(a). The policy of the MRT scheme is to utilize the the designed RTS packet (called M-RTS) that will be specified and destined to more than one receiver, i.e. to the multiple receiver set $\mathbf{R}_M$ where M denotes the maximal number of receivers that will be specified within the M-RTS packet. In other words, additional receivers within the neighbor table $\mathbf{T}_{N_i}$ will be randomly chosen to accept the M-RTS packet other than the original targeting node that is located within the set $\mathbf{B}$, i.e. the value of M is designed to be always greater than one. In comparison with the original RTS packet, there is an additional CTS responding list in the M-RTS packet. This CTS responding list records the order of response for each receiver in $\mathbf{R}_M$, which ensures that the M receivers can arrange their CTS responses without collisions. Therefore, the probability for all N_i's receiving nodes to

13
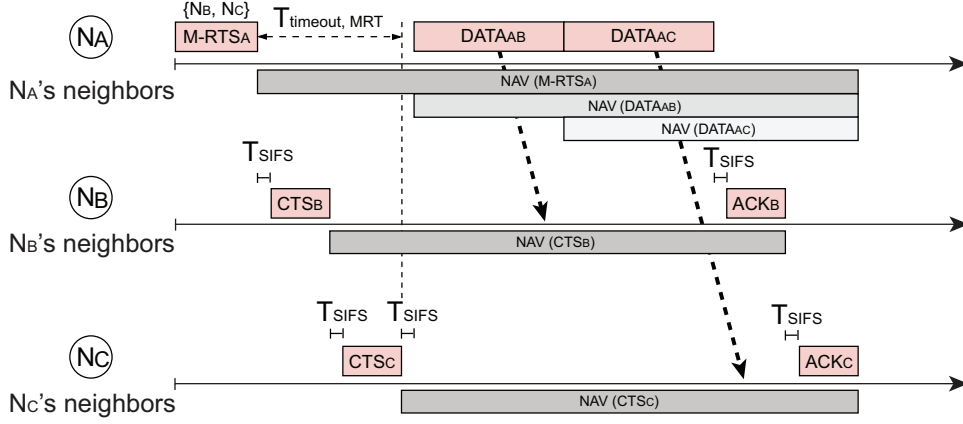
Figure 4.1: The data delivery process of the proposed MRT mechanism.

be blocked will be reduced from p_f to p_f^M, where $0 \leq p_f < 1$ is denoted as the probability of transmission failure. Consequently, the receiver blocking problem can be alleviated, which results in the enhancement of network throughput.

Fig. 4.1 shows the exemplified timing diagrams for the proposed MRT scheme. It is assumed that N_A wins the contention for channel access and is ready to transmit its data packets, where the maximal number of receivers within the multiple receiver set $\mathbf{R}_M$ is chosen as $M = 2$. First of all, the ideal case is considered where none of the selected node for $\mathbf{R}_M$ is located within the set $\mathbf{B}$, e.g. $\mathbf{R}_M = \{N_B, N_C\}$ as shown in Fig. 3.1(a). Based on the proposed MRT scheme, N_A will therefore transmit an M-RTS packet, i.e. the M-RTS$_A$ packet, which targets to both the two receivers N_B and N_C. Under the case with non-blocking receivers, N_B and N_C will sequentially feedback their CTS packets to N_A with the time difference of T_{SIFS}, where the order of the CTS feedbacks is specified within the M-RTS$_A$ packet. After the reception of the CTS$_B$ and CTS$_C$ packets, N_A will start the delivery of data packets to both N_B and N_C, respectively. Finally, the two receiver nodes will acknowledge the data packets by the corresponding ACK packets,

14

i.e. ACK_B and ACK_C.

On the other hand, the receiver blocking problem can happen when one of the selected nodes in $\mathbf{R}_M$ belongs to the set $\mathbf{B}$, e.g. $\mathbf{R}_M = \{N_B, N_3\}$. Similar to the explanation as in Fig. 4.1, N_A will initiate the M-RTS$_A$ packet that is addressed to both N_B and N_3. In this case, N_A will not receive the CTS packet from N_3 since N_3 is within the receiver blocking group $\mathbf{B}$. Therefore, the data packet towards N_B will be transmitted after the end of two CTS response time since the MRT protocol needs to wait for the required response time from the selected destinations. Afterwards, N_B will send the ACK packet if it successfully receives the data packet from node N_A. In the case that N_A does not receive any CTS feedbacks, N_A will re-initiate the contention process after a timeout period, which is M multiple of the original length defined in the conventional IEEE 802.11 protocol, i.e. $T_{timeout,MRT} = M \cdot T_{timeout}$.

4.2 Fast NAV Truncation (FNT) Scheme

The design concept of the proposed FNT mechanism is to increase the probability of channel contention under the occurrence of the receiver blocking problem. Note that the FNT scheme is designed independently but can be combined with the MRT protocol. Considering the same case that N_A intends to transmit data packets to N_3 as shown in Fig. 3.1(a), it can be observed that N_A will continue to win the channel contention on those retrials to N_3 since all the other nodes will consistently be set at their NAV states. As shown in Fig. 3.1(b), the NAV timer assigned by N_A is longer enough to prevent the other competitors from contending the channel during its retransmission to the node in receiver blocking group $\mathbf{B}$. In order to provide the channel accessing opportunities for the competitors, the proposed
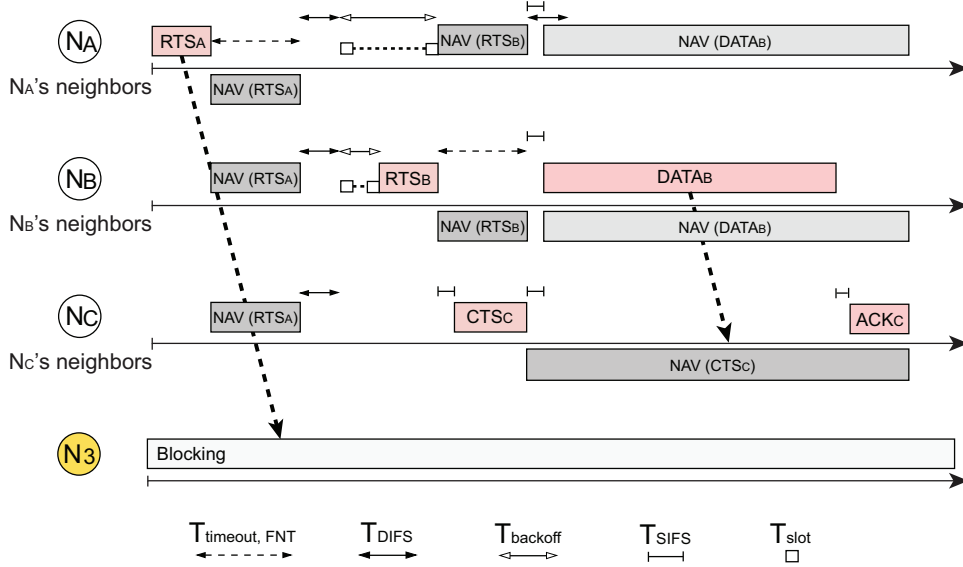
Figure 4.2: The timing diagrams of N_3, N_A, N_B, and N_C under the proposed FNT mechanism: The nodes (N_A, N_3) and (N_B, N_C) are the two transmission pairs, where N_A and N_B are the two corresponding source nodes. N_A's data transmission fails since N_3 is in the receiver blocking group **B**. Thanks to the proposed FNT mechanism of truncating the NAV timer, N_B can initialize the channel contention and win the channel to start the data transmission for N_C.

FNT scheme reduces the NAV duration specified within the RTS packet to a shorter period of time which only protect until the end of current transmission of the CTS packet, i.e. a NAV duration of $T_{NAV,FNT} = T_{SIFS} + T_{CTS} + T_{prop}$ will be set within the RTS packet based on the FNT scheme.

As shown in Fig. 3.1(a) and Fig. 4.2, N_A and N_B are ready to contend the channel for delivering their data packets to the destination nodes N_3 and N_C, respectively. It is assumed that N_A succeeds in the channel contention and starts to communicate with N_3 by sending the RTS packet, i.e. the RTS$_A$. Based on the proposed FNT scheme, both N_B and N_C will terminate the channel contention process by setting their corresponding NAV timers

16

to a duration of $T_{NAV,FNT}$. In the meantime, N_A will continue to wait for the response, i.e. the CTS packet, that is supposed to be initiated from N_3. However, since N_3 is located within the receiver blocking group **B**, none of the CTS packet will be generated in the time interval of $T_{timeout,FNT} = T_{SIFS} + T_{CTS} + T_{prop}$ by N_3 in response to N_A's data transmission request. It's noted that the duration of $T_{timeout,FNT}$ and $T_{NAV,FNT}$ is truncated to the same length in the proposed FNT protocol. Therefore, all the three nodes N_A, N_B, and N_C are free to contend the channel after the time period $T_{timeout,FNT}$, and both N_A and N_B will restart the channel contention process with equal channel accessing opportunities.

After the second round of channel contention as shown in Fig. 4.2, it is assumed that N_B succeeds in the possession of the channel and constructs the communication links with node N_C by the transmission of the RTS packet, i.e. the RTS_B packet. Similarly, based on the FNT scheme, N_A will set up its NAV timer for a period of $T_{NAV,FNT}$ preventing itself from contending the channel. As N_B receives the CTS response from N_C, N_B will start to deliver the data packets to N_C after a period of time T_{SIFS}. It is noticed that N_A will not interfere with the data delivery process of N_B since the waiting time of T_{DIFS} for starting the channel contention process is comparably larger than the waiting time T_{SIFS} for initializing the delivery of data packets. Furthermore, a NAV timer will be set to N_A, i.e. NAV($DATA_B$) as shown in Fig. 4.2, until the end of the packet delivery and acknowledgement between N_B and N_C. Consequently, the receiver blocking problem can be effectively alleviated by adopting the proposed FNT scheme.

4.3 Adaptive Receiver Transmission (ART) Scheme

As described in section 4.1, the main concept of the MRT protocol is similar to the adoption of multi-user diversity in order to alleviate the effect of receiver blocking problem. However, the MRT scheme will confront the inefficiency problem due to the requirement to allow a large amount of sequential feedbacks from the CTS packets. The major reason is that the MRT protocol has to wait for the response time of all the CTS packets from the selected destinations even though those nodes may not be able to reply with the CTS packets. This drawback can become more severe especially under the situation that the maximal number of receivers M specified within the M-RTS packet is designed to be a large value. Furthermore, as there are more than one receivers replying the CTS packets to the corresponding M-RTS transmission, the data transmission delay of these selected receivers will be increased since each receiver will spend time waiting for the data packets that are not destined to itself until the end of the entire data transmission. As shown in Fig. 4.1, after N_A receives the CTS responses from N_B and N_C sequentially, the data packet $DATA_{AB}$ will firstly be delivered from N_A to N_B. During this time period, N_C has no choice but to wait until the end of $DATA_{AB}$ transmission since the channel around N_C's coverage is already reserved. Similarly, when N_C is receiving the data packet $DATA_{AC}$ from N_A, N_B can not acknowledge the data packet via the corresponding ACK packet even though N_B has already received its data packet. Therefore, the system throughput can be limited by adopting the MRT scheme, which initiates the design of ART protocol.

In order to alleviate the problem associated with the MRT scheme, the proposed ART protocol is designed to enhance the system throughput by
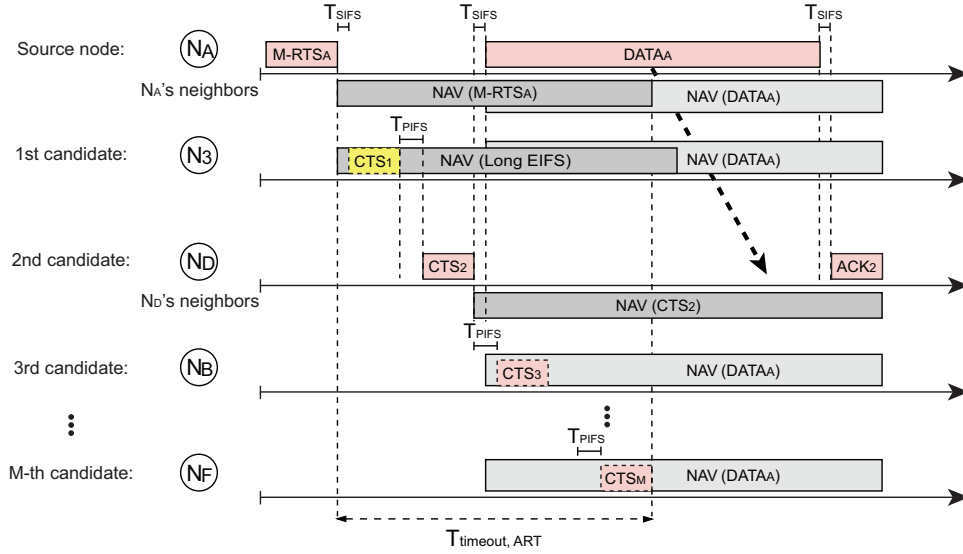
Figure 4.3: The timing diagram for the ART protocol: If N_3 cannot correctly receive the M-RTS packet from N_A, it will set its NAV timer as $T_{LongEIFS}$ in order not to interfere the CTS reception of other nodes. After waiting for N_3's required CTS response time along with T_{PIFS}, N_D replies with a CTS packet and further triggers the data transmission. The other destination nodes will suspend their CTS feedbacks to N_A.

conducting opportunistic CTS feedback. As shown in Fig. 4.3, N_A initiates the communication to the designated M receivers by broadcasting the M-RTS packet to its neighbors. Based on the order of receivers specified in the M-RTS packet from N_A, these M destinations are designed to potentially reply their corresponding CTS packets to N_A sequentially. One of the major design parameters in the ART scheme is that the inter-frame space between two CTS packets is modified from T_{SIFS} to $T_{SIFS} + T_{slot}$, which is coincidentally equal to the point coordination function (PCF) inter-frame space T_{PIFS}. Note that the adoption of $T_{PIFS} = T_{SIFS} + T_{slot}$ in the proposed ART scheme will not conflict with the original centralized PCF coordination since only ad-hoc operations are considered in the network. The reason to

19

wait for additional T_{slot} within the T_{PIFS} is to allow the receivers to verify if they should continue transmitting their CTS packets. Since each receiver may not be able to hear the CTS feedbacks from other receivers to N_A, an elongated waiting time interval T_{PIFS} is required for each receiver to ensure if there exists data transmission from N_A to its pervious receiver after a successful M-RTS/CTS negotiation. If a receiver does not hear the CTS transmission associated with the data packet from N_A to its previous receiver after time T_{PIFS}, the receiver will initiate the delivery of a CTS packet to N_A to request for data transmission. On the other hand, with successful M-RTS/CTS handshaking between N_A and the previous receiver, the data packet from N_A can therefore be transmitted after the short time duration T_{SIFS}. Consequently, by observing the on-going data transmission during the additional T_{slot} time interval, the remaining receivers will suspend their CTS feedbacks to N_A in order to prevent unnecessary channel reservation within their transmission ranges.

According to the mechanism as stated above, there is only one selected receiver that replies its CTS packet back to N_A, which consequently can reduce the waiting time for other data packets that are not destined to itself. Similar to the other non-destination neighbors, those unselected destinations must wait for the NAV period until the end of on-going communication. Note that if a node can correctly receives the M-RTS packet, it will set up its NAV timer for the time period as

$$T_{NAV,ART} = T_{SIFS} + (M-1)T_{PIFS} + M(T_{CTS} + T_{prop}) \qquad (4.1)$$

Furthermore, N_A will re-initiate the contention process after $T_{timeout,ART} = T_{NAV,ART}$ if N_A does not receive any CTS feedbacks, which is inherited from the FNT scheme proposed in the previous section. After data packet has been

designated to a specific receiver, the other non-selected receivers and non-destination neighbors will refresh their NAV period to become $T_{Data}+T_{SIFS}+T_{ACK}+2T_{prop}$ until the data has completed its transmission. Therefore, the channel can be completely reserved within the transmission range of a source node, and the channel reservation becomes more flexible if the source node fails to establish the link with its receivers in this round of transmission.

In certain situations, the receivers may receive scrambled signals that can not be decoded such that the M-RTS packet delivered from N_A will not be correctly received, e.g. the receiver N_3 as shown in Fig. 4.3. The reason is that these receivers are located in the receiver blocking group **B** where some neighbor nodes are simultaneously transmitting their packets. Therefore, in order not to interfere with either the CTS or ACK reception of other source nodes, N_3 is designed to wait for a longer NAV duration as long EIFS that can be obtained as $T_{LongEIFS}=T_{SIFS}+(M-1)T_{PIFS}+M(T_{CTS}+T_{prop})+T_{DIFS}$, which is extended from the conventional $T_{EIFS}=T_{SIFS}+T_{CTS}+T_{prop}+T_{DIFS}$ in the IEEE 802.11 system. Even if N_3 can correctly receive the M-RTS packet from N_A, N_3 may not be able to reply its corresponding CTS packet since it can be NAVed by other on-going transmission in its neighborhood. N_3 will be requested to refresh its NAV timer for $T_{NAV,ART}$ similar to the other non-destination neighbors of N_A. Furthermore, consider a node, e.g., N_B, correctly receives the M-RTS packet from a source node N_A, and is notified to be one of the M receivers. During the time interval between the end of M-RTS transmission and before its CTS feedback, N_B may receive other M-RTS or CTS packets from its neighbors before N_B to broadcast its corresponding CTS packet to the original source node N_A. Under such situation, no matter if N_B will be informed to be the receiver from other source nodes, N_B will be requested to set its corresponding NAV timer according to the newly received M-RTS or CTS packet, which results in the termination of its original CTS

feedback.

Referring to Fig. 4.3 as an example, it is assumed that N_A wins the contention for channel access and transmits its M-RTS packet to M destinations. All of N_A's neighbors will set their NAV period to be $T_{NAV,ART}$. Consider the case that N_3 is unable to receive the M-RTS packet correctly from N_A, N_3 will adjust its NAV timer as $T_{LongEIFS}$ in order not to interfere with the other transmissions in the network. After waiting for the time durations of both CTS_1 transmission and T_{PIFS}, N_D will reply with its CTS feedback, i.e. CTS_2, to N_A to request for data transmission. After observing the CTS_2 packet from N_D, the other nodes within the transmission range of N_D will set their NAV period to be $T_{Data} + T_{SIFS} + T_{ACK} + 2T_{prop}$ which is the same as that in the duration field of conventional CTS packet. As N_A has received its first CTS feedback from N_D, N_A will begin the data transmission to N_D after the time duration of T_{SIFS}. The CTS feedbacks from the other destinations, i.e. from third candidate to M-th candidate, back to N_A will therefore be suspended. After the successful data transmission, the corresponding ACK packet, i.e. ACK_2, will be acknowledged from N_D to N_A.

4.3.1 Dynamic Adjustment of Parameter M in the ART Protocol

The maximal number of receivers M for each sending node should be determine in order to feasibly improve the network performance. The proposed ART scheme allows each node to maintain and dynamically adjust its own value of parameter M based on the real-time network environment. In order to further identify the dynamic behavior of parameter M, it will be modified as M_i where $i = 1$ to N with N denoting the total number of nodes in the network. Fig. 4.4 shows the algorithm for dynamically adjusting the
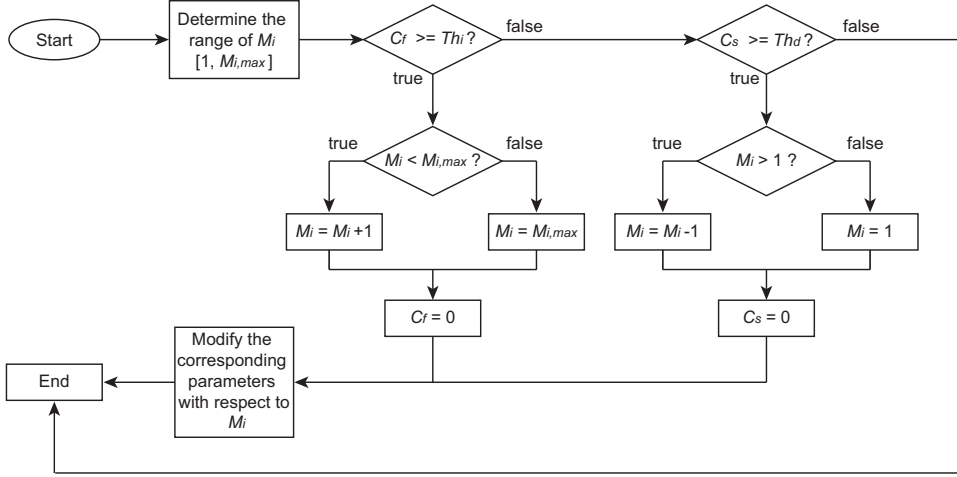
Figure 4.4: The flow chart for dynamic adjustment of parameter M_i by adopting the ART protocol.

parameter M_i at every node in the network. As a node wins the contention for channel access, e.g. node N_i, it will execute the algorithm to determine the value of M_i in this transmission round before broadcasting its M-RTS packet. First of all, the range of M_i for N_i will be determined for the dynamic adjustment algorithm as $[1, M_{i,max}]$, where the maximum value of this range $M_{i,max}$ can be obtained as

$$M_{i,max} = \min\{\omega_i, n_i\} \tag{4.2}$$

Note that the parameter n_i denotes the total number of neighbor nodes of N_i. The other parameter ω_i in (4.2) is utilized to limit the length of NAV timer of N_i's neighbor nodes not to exceed the best case of a successful data transmission. In other words, according to (4.1), the NAV duration for those unselected destination nodes after receiving the M-RTS packet from N_i will be constrained to be $T_{NAV,ART} = T_{SIFS} + (\omega_i - 1)T_{PIFS} + \omega_i(T_{CTS} + T_{prop}) \leq 3T_{SIFS} + T_{CTS} + T_{Data} + T_{ACK} + 3T_{prop}$. Consequently, the parameter ω_i will

be selected as

$$\omega_i = \left\lfloor \frac{2T_{SIFS} + T_{PIFS} + T_{CTS} + T_{Data} + T_{ACK} + 3T_{prop}}{T_{PIFS} + T_{CTS} + T_{prop}} \right\rfloor \qquad (4.3)$$

Note that the main purpose of the minimization in (4.2) is to intuitively constrain the parameter ω_i derived from NAV duration not to exceed the total number of neighbors n_i of N_i.

As depicted in the flow chat as shown in Fig. 4.4, the dynamic adjustment of parameter M_i will first verify with an increasing threshold Th_i to determine if the current M_i should be increased or not. The verification criterion is based on the number of continuously transmission failure of the M-RTS packets from the previous rounds, which is denoted as C_f. If C_f is greater than Th_i, the adjustment algorithm considers this situation as potential occurrence of receiver blocking problem. In general, the probability of continuously M-RTS collisions will be small since the BEB mechanism can adequately avoid packet collision if there does not exist the receiver blocking problem. Therefore, the algorithm is designed to increase the current M_i value such that there will be additional receivers to assist the data delivery process from the source node. As shown in the left part of the flow chat in Fig. 4.4, the current M_i value will be verified whether it is less than the maximum value $M_{i,max}$. If the condition is true, the current value of M_i will be increased by one; otherwise, M_i is set equal to $M_{i,max}$. Consequently, the counter C_f will be reset to zero to initiate another accumulation of M-RTS transmission failures.

On the other hand, if C_f is less than the increasing threshold Th_i, the right part of the flow chart will be executed. In this case, the design consideration is to examines whether the current M_i value should be decremented if the number of continuously successful data transmission, indicated as C_s, is

24

greater than the decreasing threshold Th_d. The reason is that larger value of M_i corresponds to excessive receivers are selected which can cause long delay of the corresponding CTS feedbacks. If $C_s \geq Th_d$ and $M_i > 1$, the current M_i value will be counted down by one. Furthermore, if both $C_f < Th_i$ and $C_s < Th_d$, the current value of M_i will remain the same after executing the adjustment algorithm. After the new M_i value is determined, the parameters associated with M_i will be adjusted accordingly such as M-RTS packet size, $T_{NAV,ART}$, and $T_{LongEIFS}$ for node N_i. Afterwards, the ART protocol will be adopted in N_i by broadcasting its M-RTS packet to those designated M_i receivers for packet delivery.

Chapter 5

Throughput Analysis for ART Protocol

In this chapter, throughput analysis will be performed to provide the mathematical modeling of proposed ART protocol. As shown in Fig. 5.1, Bianchi [43] has established a two-dimensional Markov chain to describe the state transition of a node where the state of each node is composed by the current retransmission stage and the current backoff window size. Every data packet will be transmitted if the backoff window size is counted down to zero value. Let the probability p denote a source node that fails in transmitting its packet; while $(1 - p)$ indicates the successful transmission probability. The two-dimensional Markov chain will return to its initial state if packet is successfully transmitted in each node. Otherwise, each node will increment its retransmission stage by one, and randomly determine its current backoff size from the corresponding contention window size based on the BEB mechanism. Consider a saturated node that always has packets to transmit, the stationary transmission probability τ at a randomly selected time slot can
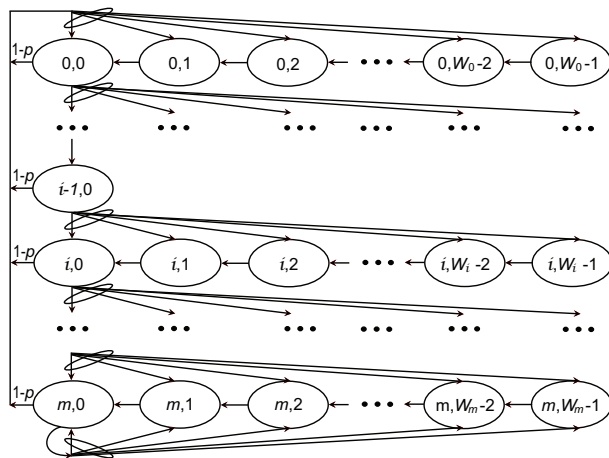
Figure 5.1: Two-dimensional Markov chain for contention-based state transition.

be obtained from the two-dimensional Markov chain as

$$\tau = \frac{2(1 - 2p)}{(1 - 2p)(W_0 + 1) + pW_0[1 - (2p)^m]} \tag{5.1}$$

where W_0 denotes the minimal contention window size and m is maximum number of retransmissions. Note that the parameter τ in (5.1) can also be translated as the probability that a node will transmit a frame in a given time slot; while $(1-\tau)$ represents the probability for a node to remain silent. Detailed derivation can also be referenced from [43].

Therefore, the relationship in (5.1) between τ and p can be adopted to other random access based MAC protocol with saturated nodes, i.e., it can be applied to the proposed ART scheme. In order to solve this non-linear equation, an additional relationship between p and τ should be acquired such that both values can be solved by adopting numerical methods. In the following sections, how the stationary transmission probability τ affects the parameter p will be investigated in multi-hop ad-hoc network with the existence of hidden terminals.

27

5.1 Network Scenario for Throughput Analysis

As adopted in the IEEE 802.11 standard, the four-way handshaking mechanism, i.e. RTS-CTS-DATA-ACK packet exchanges, is considered in the network scenario. Due to the hidden terminal problem, there is no guarantee to successfully transmit the CTS, DATA, and ACK packets in the multi-hop ad-hoc networks even if an RTS packet can be successful delivered. Furthermore, throughput performance can be severely degraded owing to the receiver blocking problem, which may requires an extra transmission hop for a packet to reach its destination. Note that routing algorithms can affect the system performance for determining the next transmission hop. In order to simplify the analysis, the proposed analytical model for the ART scheme will focus on the receiver blocking problem regardless of the adoption of specific routing algorithm. All the data packets generated from a source node are assumed to be transmitted to its network neighbors and fixed number of specific receivers are randomly selected.

Moreover, all the network nodes are randomly distributed in a two-dimensional limited area. It is assumed that the active nodes always have data packets to deliver, and the packets size are considered to be the same. In order to simplify the analysis of the ART protocol, the transmission, sensing, and interference ranges for all the network nodes are assumed equal to R; while both the capture and shadowing effects are not considered for the network channel. The transmission failure at the receiver only occurs by packet collision while there are packets simultaneously delivered by other nodes which locate within the transmission range of the receiver. Owing to packet collision, those packets that cannot be decoded must be retransmitted. The transceiver equipped in each node operates in the half-duplex
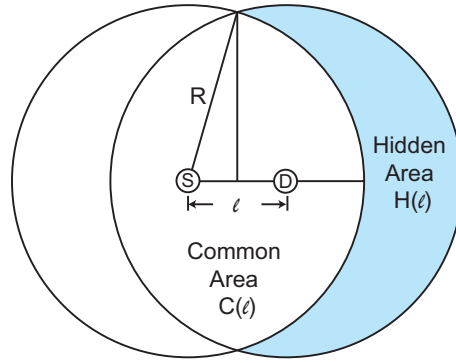
Figure 5.2: Hidden and common areas of a transmission pair in multi-hop ad-hoc network.

mode, and each node only possesses a single omnidirectional antenna.

As shown in Fig. 5.2, given the transmission pair S and D with distance ℓ apart, $C(\ell)$ represents the common area intersected by the transmission ranges of S and D. On the other hand, consider a tagged node S, the hidden area $H(\ell)$ is defined as the area enclosed by D's transmission range excluding the common area $C(\ell)$. Consider S as the transmitter for packet delivery, its M-RTS packet may not only incur packet collision within its own coverage but also suffer from transmission failure from potential hidden nodes in its hidden area $H(\ell)$. Similarly, some neighbors of node D may not be able to correctly receive the CTS packet from the receiver D since there can exist a transmission pair in D's hidden area, and the following data delivery between S and D will potentially be collided by these neighbor nodes of receiver D. Since the nodes are uniformly distributed in a constrained area with radius R, the distance between the tagged node S and its neighbor D will become a random variable L. Note that ℓ denotes one of the specific outcomes of L for $0 \leq \ell \leq R$. The probability density function (PDF) $f_L(\ell)$ of the random

29

variable L can be obtained as

$$f_L(\ell) = \int_0^{2\pi} f_{L,\Theta}(\ell,\theta)d\theta = \int_0^{2\pi} f_{X,Y}(\ell\cos\theta, \ell\sin\theta) \cdot |J(\ell,\theta)|d\theta = \frac{2\ell}{R^2} \quad (5.2)$$

where $f_{X,Y}(x,y) = f_{X,Y}(\ell\cos\theta, \ell\sin\theta) = 1/(\pi R^2)$. The parameters X and Y are the random variables in the cartesian coordinates, L and Θ are the corresponding random variables in the polar coordinates, and $J(\ell,\theta)$ denotes the Jacobian matrix. In order to estimate the impact of hidden terminals, it is required to calculate the size of region where possible hidden terminals may exist. First of all, given the distance ℓ, the common area can be computed based on geometric relationship as $C(\ell) = 2R^2 \arccos(\frac{\ell}{2R}) - \ell(R^2 - \frac{\ell^2}{4})^{1/2}$. Consequently, the hidden area $H(\ell)$ can be obtained as

$$H(\ell) = \pi R^2 - C(\ell) = \pi R^2 - 2R^2 \arccos\left(\frac{\ell}{2R}\right) + \ell\left(R^2 - \frac{\ell^2}{4}\right)^{\frac{1}{2}} \quad (5.3)$$

Based on (5.2) and (5.3), the average value of hidden area A_h can be expressed as

$$A_h = \int_0^R f_L(\ell)H(\ell)d\ell = \frac{2}{R^2}\int_0^R \ell H(\ell)d\ell \quad (5.4)$$

and the average value of common area is acquired as $A_c = \pi R^2 - A_h$.

5.2 Behavior of Tagged Node S

The analytical model for throughput performance will be derived based on the standpoint of a tagged node. As shown in Fig. 5.2, the tagged node S intends to establish network connection with its neighbor node D. There are three possible states that can happen to node S in a given time slot as follows: (a) In the silent state, S may start to count down its backoff timer after the channel has been sensed idle. On the other hand, it can be

notified to freeze its backoff timer for a NAV duration due to either the PCS or VCS mechanism since there may exist either a transmitter or a receiver communicating within its coverage. (b) In the successful transmission state, after the backoff counter has reached zero, S will start its transmission and finally successfully transmit the data packets. (c) In the transmission failure state, S will suffer from packet collisions either via the other transmissions within its coverage or via the interference by the hidden nodes. Note that (5.1) can consequently be solved if the probability of failure transmission can be formulated while S is in the transmission failure state as (c). After formulating the probabilities for the tagged node S to be at one of the three states (a), (b), and (c), the throughput performance of S can therefore be calculated.

On the other hand, it is more complex to compute the successful transmission probability since there are more events needs to be considered. Given the tagged node S initiating communication by broadcasting an M-RTS packet in a given time slot, the transmission will be successful to an arbitrary intended receiver D if and only if all of the following events hold: (i) There does not exist a node in D's coverage that transmits the M-RTS packet during the same slot time; (ii) None of the nodes in D's coverage transmits the CTS packet in the same slot time; (iii) None of the nodes are involved in communication in the hidden area A_h of S during node S's M-RTS transmission time. Otherwise, receiver blocking problem can be occurred; and (iv) All the nodes in D's coverage can correctly receive the CTS packet from D, and consequently setup their NAV vectors. Otherwise, these nodes can interfere with D by transmitting their M-RTS packets or replying the CTS packets. However, the interference from this type of nodes to D is in general considered limited such that event (iv) will not be considered in the performance analysis for simplicity purpose. Moreover, since the CTS packet is triggered

by its corresponding successfully transmitted M-RTS packet, the influence from the CTS transmission is relatively smaller than that from the M-RTS packets. Therefore, the effect from the CTS packets as stated in (ii) will not be considered in the analysis. In the next three subsections, the three states of a tagged node S in a particular time slot will be described as follows.

5.2.1 S in Silent State

There are three different network scenarios that need to be considered if the tagged node S is in the silent state as follows. Case 1: All nodes within the carrier sensing range of S will not conduct any packet transmission; Case 2: Only one node exists in the carrier sensing range of node S transmitting packets; and Case 3: Two or more nodes in the carrier sensing range of node S conduct packet transmission. With the definition of transmission probability τ, the probability for S to be in the silent state in a considered slot time becomes $1 - \tau$. The probability that all the neighbors of S are in the silent state can consequently be obtained as $(1-\tau)^{n-1}$, where $n = \rho \pi R^2$ represents the average number of nodes in S's carrier sensing range and ρ denotes the node density with unit as number of nodes per meter square. Therefore, the probability for Case 1 to happen can be obtained as $P_{i,1} = (1 - \tau)^n$. The tagged node S will remain in the silent state for the duration of a slot time T_{slot}, and consequently decrement its backoff window size by one.

Furthermore, consider the situation that there exists at least one node intending to transmit data within the carrier sensing range of S. The corresponding conditional probability that only one node, e.g. N_x, is conducting data transmission can be obtained as

$$P_t = \frac{(n - 1)\tau(1 - \tau)^{n-2}}{1 - (1 - \tau)^{n-1}} \tag{5.5}$$

In Case 2, it is required to consider two scenarios that only node N_x can either success or fail in its transmission. First of all, the probability for N_x to successfully transmit its packet is acquired as

$$P_{i,2s} = \left[(1 - \tau) \left(1 - (1 - \tau)^{n-1} \right) P_t \right] (1 - p) \qquad (5.6)$$

Note that p indicates the probability of failure transmission as was defined previously. On the other hand, after the backoff timer of S is suspended, the total time duration for this case can be acquired as

$$T_{i,2s} = T_{mRTS} + \overline{T}_{CTS} + T_{Data} + T_{ACK} + 3T_{SIFS} + 3T_{prop} + T_{DIFS} \qquad (5.7)$$

where T_{mRTS} and $\overline{T}_{CTS}$ are the time durations for the M-RTS transmission and the required average time for receiving a correct CTS packet, respectively. In order to obtain the value of $\overline{T}_{CTS}$, it is required to firstly calculate the probability of failure transmission caused by one of the M attempts from the M-RTS packet as

$$P_\psi = \left[1 - (1 - \tau)^{n_c - 1} \right] + (1 - \tau)^{n_c - 1} P_{hd} \qquad (5.8)$$

where the first term represents the collision probability that at least one node transmits in the common area A_c of N_x, and $n_c = \rho A_c$ indicates the average number of nodes in A_c. The second term denotes the failure probability caused by hidden terminals where the probability P_{hd} can be calculated as $P_{hd} = 1 - (1 - \tau)^{n_h \zeta_v}$ with the parameter $n_h = \rho A_h$ representing the average number of nodes in the hidden area of N_x. The probability P_{hd} represents at least one node in the hidden area A_h of N_x that is not in the silent state during the vulnerable period ζ_v, which can be computed as $\zeta_v = \left\lceil \frac{T_{mRTS} + T_{prop} + T_{SIFS}}{T_{slot}} \right\rceil$ with the unit as number of slots. Note that the term $(1 - \tau)^{n_h \zeta_v}$ denotes the

probability for all nodes within N_x's hidden area which are in the silent state during the vulnerable period. It is assumed that the connection is established until the kth CTS packet is successfully transmitted, where k denotes a value of random variable K which follows the geometric distribution. Based on (5.8), the average number of CTS packets that are successfully transmitted can be obtained as

$$\overline{n}_{CTS} = \sum_{k=1}^{M} k P_\psi^{k-1}(1 - P_\psi) \tag{5.9}$$

Therefore, according to (5.9), the average time duration to receive a correct CTS packet $\overline{T}_{CTS}$ becomes

$$\overline{T}_{CTS} = \overline{n}_{CTS}(T_{CTS} + T_{prop}) + (\overline{n}_{CTS} - 1)T_{PIFS} \tag{5.10}$$

Note that (5.10) can therefore be substituted into (5.7) for the computation of $T_{i,2s}$. On the other hand, the other scenario is to consider the probability that N_x fails in transmitting its packets, which can be expressed similar to (5.6) as

$$P_{i,2f} = \left[(1 - \tau)\left(1 - (1 - \tau)^{n-1}\right) P_t \right] p \tag{5.11}$$

Based on the proposed ART scheme, the associated time duration for S to freeze its backoff timer can be acquired as

$$T_{i,2f} = T_{mRTS} + T_{prop} + T_{NAV,ART} + T_{DIFS} \tag{5.12}$$

where $T_{NAV,ART}$ is depicted in (4.1) for the proposed ART protocol. Furthermore, in Case 3, the probability for two or more neighbor nodes of S to transmit data in a given time slot can be formulated as

$$P_{i,3} = (1 - \tau)\left[1 - (1 - \tau)^{n-1}\right](1 - P_t) \tag{5.13}$$

Since S will receive more than one M-RTS packets simultaneously transmitting in the given time slot, only the scrambled signals will be acquired by S. In order to prevent from interfering the reception of either the CTS or the ACK packets at other source nodes, S is designated to setup its NAV period as long EIFS time duration. Therefore, the total required time interval for S in Case 3 by adopting the ART protocol can be acquired as

$$T_{i,3} = T_{mRTS} + T_{prop} + T_{LongEIFS} \tag{5.14}$$

Node S will continue to countdown its backoff timer after this time duration.

5.2.2 S in Successful Transmission State

The main target of proposed ART scheme is to adaptively increase the multi-user diversity in order to improve the throughput performance. With the transmission probability τ of S in a given slot time, a specific round of M-RTS transmission is considered unsuccessful only if all the attempts fail to receive the CTS packets from those M designated receivers. Therefore, the probability for S to be in the successful transmission state can be approximated as

$$P_s \cong \tau(1 - P_\psi^M) \tag{5.15}$$

where P_ψ denotes the failure transmission probability caused by one of the M attempts as can be obtained in (5.8). Note that the approximation in (5.15) holds under the condition that the number of receiver M is not too large such that the candidate receivers in the coverage area will not correlate with each other. Moreover, the total time duration for S to successfully transmit its data packet can be expressed as

$$T_s = T_{mRTS} + \overline{\overline{T}}_{CTS} + T_{Data} + T_{ACK} + 3T_{SIFS} + 3T_{prop} + T_{DIFS} \tag{5.16}$$

where the average time duration for receiving a correct CTS packet $\overline{T}_{CTS}$ can be obtained from (5.10).

5.2.3 S in Transmission Failure State

Consider the tagged node S stays in the transmission failure state given the transmission probability τ in a given time slot, there are two cases that can happen as follows: (a) Packet collision of the M-RTS transmission occurs in the common area A_c of S, and (b) Failure transmission of M-RTS packet happens from the influence of hidden nodes in A_h of S during the vulnerable period ζ_v. In Case (a), the collision probability can intuitively be formulated with the adoption of ART scheme as

$$P_{f,c} \cong \tau \left[1 - (1 - \tau)^{n_c - 1} \right]^M \tag{5.17}$$

Note that the transmission failure in this case indicates that all of the M transmission attempts to the designated receivers are collided in A_c of S within a given slot time. The required time duration for the tagged node S to spend in this event can be obtained as

$$T_{f,c} = T_{mRTS} + T_{prop} + T_{LongEIFS} \tag{5.18}$$

On the other hand, if at least one of the M attempts is not collided in A_c of S, the transmission failure can still occur due to the potential packet delivery of hidden nodes in A_h of S. The failure transmission probability under this circumstance, i.e. Case (b), can therefore be approximately computed as

$$P_{f,h} \cong \tau \left[\sum_{i=1}^{M} C_i^M \left[(1 - \tau)^{n_c - 1} \right]^i \left[1 - (1 - \tau)^{n_c - 1} \right]^{M-i} P_{hd}^i \right] \tag{5.19}$$

36

where C_i^M represents the binomial coefficient. The required time duration for S to spend under this case can be expressed as

$$T_{f,h} = T_{mRTS} + T_{prop} + T_{timeout,ART} + T_{DIFS} \qquad (5.20)$$

Finally, combining (5.17) and (5.19), the probability of transmission failure in a particular round of attempt can be expressed as

$$p = \frac{P_{f,c} + P_{f,h}}{\tau} \qquad (5.21)$$

which indicates the conditional probability that there is transmission failure given the tagged node S transmits in a considered slot time. Therefore, combining the nonlinear equations (5.1) and (5.21), the parameters τ and p can be iteratively solved by adopting numerical methods. After the failure transmission probability p is obtained, the probability $P_{i,2s}$ in (5.6) and $P_{i,2f}$ in (5.11) can also be determined. All the events discussed above are summarized in Table 1.

The system throughput is defined as the number of bits in the data payload that are successfully transmitted per unit time, which represents the throughput per hop of a single node in the multi-hop ad-hoc networks. Based on the probabilities obtained in Table 1, the throughput Φ can consequently be acquired as

$$\Phi = \frac{8L \cdot P_s}{P_{i,1}T_{slot} + P_{i,2s}T_{i,2s} + P_{i,2f}T_{i,2f} + P_{i,3}T_{i,3} + P_sT_s + P_{f,c}T_{f,c} + P_{f,h}T_{f,h}} \qquad (5.22)$$

where L denotes the total number of bytes in the payload. Furthermore, for evaluation purpose, the throughput performance of the conventional IEEE 802.11 multi-hop ad-hoc networks can also be acquired with several modifi-

TABLE 1

Summary for the probability of seven events at a considered slot of time

Prob.	Value of the probability	Time	Result
$P_{i,1}$	$(1-\tau)^n$	T_{slot}	Backoff
$P_{i,2s}$	$\left[(1-\tau)\left(1-(1-\tau)^{n-1}\right)P_t\right](1-p)$	$T_{i,2s}$	Freeze its backoff timer
$P_{i,2f}$	$\left[(1-\tau)\left(1-(1-\tau)^{n-1}\right)P_t\right]p$	$T_{i,2f}$	Freeze its backoff timer
$P_{i,3}$	$(1-\tau)\left[1-(1-\tau)^{n-1}\right](1-P_t)$	$T_{i,3}$	Freeze its backoff timer
P_s	$\tau(1-P_\psi^M)$	T_s	Success
$P_{f,c}$	$\tau\left[1-(1-\tau)^{n_c-1}\right]^M$	$T_{f,c}$	Failure due to collision
$P_{f,h}$	$\tau\left[\sum_{i=1}^{M}C_i^M\left[(1-\tau)^{n_c-1}\right]^i \cdot \left[1-(1-\tau)^{n_c-1}\right]^{M-i}P_{hd}^i\right]$	$T_{f,h}$	Failure due to hidden nodes

cations as follows. First of all, the parameter $M = 1$ and the probability p in (5.6) and (5.11) is set to 0. The time duration $T_{i,2s}$ in (5.7) is modified to become $T_{i,2s} = 3T_{SIFS} + T_{RTS} + T_{CTS} + T_{Data} + T_{ACK} + 4T_{prop} + T_{DIFS}$. The probability P_s in (5.15) is modified to $P_s = \tau(1-\tau)^{n_c-1}(1-\tau)^{n_h\zeta_v}$, and the corresponding T_s is revised to be same as the modified value of $T_{i,2s}$. Finally, the probability $P_{f,h}$ in (5.19) is modified to be $P_{f,h} = \tau(1-\tau)^{n_c-1}P_{hd}$. Note that the time duration $T_{LongEIFS}$ is degenerated to be T_{EIFS} since the parameter M is set to 1. Therefore, with the modifications as stated above, the system throughput for IEEE 802.11 ad-hoc networks can be obtained according the same formulation as (5.22).

Chapter 6

Performance Evaluation

The performance of the proposed schemes will be evaluated and compared via simulations. Unless additionally specified, the default settings for the simulation parameters are listed in Table 2. Note that some of the parameters in Table 2 are adopted from IEEE 802.11a standard. The network nodes are randomly distributed in a $B \times B$ square meters area, where the parameter B is denoted as the boundary limit. Note that the value of node density ρ can be obtained as $\rho = N/(B^2)$ with N as the total number of nodes in the network. Moreover, both the MAC header and the control packets, i.e. M-RTS, CTS, and ACK packets, are transmitted in basic rate; while the payload part of a data packet is delivered in data rate. In the following figures for performance evaluation, each data point is averaged from 50 simulation runs where each simulation run is executed for 50 seconds. In section 6.1, the proposed analytical model for the ART protocol is validation via simulations; while the observation on the parameter M_i is performed in section 6.2. Performance comparison between the proposed schemes and existing protocols are compared in section 6.3.

TABLE 2

Simulation parameters

Parameter Type	Parameter Value
Simulation Time	50 sec
Transmission Range (R)	30 m
Boundary Limit (B)	180 m
Max. Retrial Limit (m)	7
Min. Contention Window Size (W)	16
Total Number of Nodes (N)	60
Data Rate	24 Mbps
Basic Rate	6 Mbps
T_{SIFS}	16 μs
T_{DIFS}	34 μs
T_{PIFS}	25 μs
T_{slot}	9 μs
T_{prop}	1 μs
$T_{preamble+plcp}$	20 μs
Length of MAC header	224 bits
Length of M-RTS packet	$20 + 6(M_i - 1)$ Bytes
Length of CTS packet	14 Bytes
Length of ACK packet	14 Bytes
Payload Size (L)	3000 Bytes

6.1   Performance Validation

The analytical model presented in Chapter 5 for throughput performance of the proposed ART protocol will be validated via simulations. Figs. 6.1 and 6.2 illustrate the performance validation of the ART scheme under $M = 2$ and 4, respectively; while Fig. 6.3 shows the validation of the analytical model for conventional IEEE 802.11a DCF protocol which is described in the last paragraph of Chapter 5. The average throughput versus number of nodes (N) and data payload size (L) are shown in the left and right plots, respectively. Note that the legends "ana" indicates the data from analytical models; while "sim" represents simulation results. It can be observed that the

system throughput will be decreased with the augmentation of total number of nodes since there will be higher probability to exist hidden nodes that can cause additional packet collisions in the network. On the other hand, as the payload size is increased, enhanced throughput performance can be obtained owing to the reason that each node can transmit additional information bits after it acquires the channel access. Furthermore, it can be seen from all these figures that the results obtained from the analytical models for both ART and IEEE 802.11a DCF protocols are consistent with that acquired from simulations. Slight discrepancies are observed between the analytical and simulation results which mainly due to the assumptions and approximations adopted in the analytical models. The effectiveness of proposed analytical models can therefore be validated.

6.2 Observation on Parameter M_i

As stated in subsection 4.3.1, the number of selected receivers M_i for each source node is considered a key design parameter in the proposed ART protocol. In this section, the sensitivity of several design parameters and the observations on parameter M_i will be presented. Fig. 6.4 shows the average throughput performance versus different decreasing threshold Th_d by adopting the proposed ART scheme. The numbers of nodes are selected as $N = 40$, 80, 120, and 160. Note that the initial value of M_i in the dynamic adjustment algorithm in each node is set to be half of the average neighbor size, i.e. initial value of $M_i = \frac{1}{2}\rho\pi R^2, \forall i$. The increasing threshold Th_i is chosen to be $Th_i = 3$, which indicates that the current M_i value of the source node is increased by one if the M-RTS packet is continuously failed by three times. This selection is considered reasonable in a normal node density of network layout since the BEB mechanism can partially alleviate the packet

collision between the neighbor nodes. Therefore, the sensitivity from the decreasing threshold Th_d to the system throughput will be the major concern to be evaluated. According to Fig. 6.4, it can be observed that the system throughput will reach a constat value after the decreasing threshold has been augmented to around $Th_d = 6$ under different numbers of nodes N. In other words, this reveals the situation that a constant value of decreasing threshold Th_d can be feasibly chosen under different N values in order not to severely deteriorate the system throughput. Therefore, the increasing and decreasing thresholds are set equal to $Th_i = 3$ and $Th_d = 8$ in the following simulations for performance comparison.

Fig. 6.5 illustrates the average number of selected receivers M_i per node versus number of network nodes under payload size $L = 500, 1000, 2000$ and 4000 bytes. It can be observed that the parameter M_i will be increased with the augmentation of the number of nodes since the failure of M-RTS transmission grows with N. Consequently, the number of selected receivers M_i in each node are designed to be increased according to the dynamic adjustment algorithm as shown in Fig. 4.4. Furthermore, as defined in (4.2), the value of M_i is bounded by either the source node's neighbor size n_i or the time duration for successful data transmission represented by ω_i in (4.3). With smaller N value, the parameter $M_{i,max}$ will be potentially bounded by the neighbor size n_i; while the dominating factor will be ω_i as N becomes larger. Consequently, as the number of nodes N is increased, the saturation on the average value of M_i can be observed in Fig. 6.5 since M_i will be primarily constrained by the parameter ω_i.

6.3 Performance Comparison

In this section, the performance of proposed schemes will be compared with existing protocols including the conventional IEEE 802.11a DCF protocol, the eMAC algorithm [29], and the eDCF protocol [32]. The proposed protocols include the ART, MRT+FNT, and FNT schemes where the MRT+FNT approach denotes the combination of the MRT and FNT algorithms as described in Chapter 4. In order to provide consistent network scenario and simulation settings with the proposed schemes, each node in the eMAC protocol is selected to have the same coverage R for the transmission, sensing, and interference ranges. Therefore, the ICP frame of Type II and the out-of-band busy tone in the eMAC scheme can be ignored in the following simulations. Moreover, the overhead of eMAC-table and the data sent (DS) control frame in the eMAC protocol is assumed to be extremely small such that the best case of the eMAC scheme is evaluated in the simulations.

Fig. 6.6 shows the performance comparison between the proposed protocols and the existing schemes. In the left plot, the average throughput is compared under different number of nodes N with payload size $L = 3000$ bytes; while the throughput performance is compared under different payload sizes with $N = 60$ in the right plot. Note that the proposed ART protocol is evaluated under three cases as $M = 2$, 4, and with dynamic adjustment algorithm for M_i which is denoted as ART-DA scheme. As the total number of nodes in the network grows, it is intuitively to observe from the left plot that the throughput performance of all the schemes becomes worse since there can exist more packet collisions and additional interference from hidden nodes. The proposed ART-DA protocol can provide the highest throughput performance compared to the other schemes owing to its dynamic adjustment of selected receivers M_i. The throughput performance of eDCF protocol is similar to that of the MRT+FNT scheme since the eDCF protocol provides

a second chance to deliver the data packet to another receiver if there is no CTS feedback from the original destination. Furthermore, as the payload size becomes larger shown in the right plot, the throughput performance is increased in all the schemes since the source node is able to delivery additional information bytes after winning the channel contention. The proposed ART-DA protocol still outperform the other methods with the highest system throughput owing to its better channel utilization instead of constructing unnecessary connection attempts between the network nodes. Consequently, the simulation results show that the proposed ART protocols, especially the ART-DA scheme, can consistently outperform the other algorithms and effectively alleviate the receiver blocking problem.

Fig. 6.7 illustrates the comparison of control overhead versus number of nodes under $L = 3000$ bytes. Note that the control overhead is defined as the number of RTS/M-RTS packets over the number of CTS packets which implies the average required RTS/M-RTS packets for a protocol to acquire a CTS feedback from the selected receivers. In other words, as the control overhead is increased, the protocol will operates in a less efficient manner with worse channel utilization since it wastes excessive time in establishing the connection to obtain a CTS packet. As in Fig. 6.7, if the number of nodes is increased, additional control overhead for all the scheme can be observed which is attributed to the excessive packet collisions and retransmissions within the network. The conventional IEEE 802.11a DCF protocol results in the highest control overhead among all the schemes owing to its poor ability to handle the receiver blocking problem in the ad-hoc networks. Even though the throughput performance of the eDCF protocol is similar to that of the MRT+FNT scheme, excessive RTS packets are required by the eDCF protocol which is attributed to the second chance for delivering the data packet to another receiver that is not confirmed by the second receiver's

44

CTS packet. It can be observed that the proposed ART-DA scheme can achieve reasonable lowered control overhead compared to other protocols. With less number of network node, the behaviors of the ART-DA protocol will be similar to the cases with smaller M values, e.g. $M = 2$; while the ART-DA scheme will behave similar to the situation with larger M under increased value of N. Therefore, as can be seen from Fig. 6.7, the total number of M-RTS packets of the ART-DA protocol will intersect the curves from smaller to larger M values as the number of nodes is augmented.

Fig. 6.8 shows the performance comparison from different boundary limits B to the system throughput. As the boundary limit is less than 30 meters, the multi-hop ad-hoc network will be degenerated to be a single hop ad-hoc network. The hidden terminal problem becomes minimal where the transmission failure is primarily caused by the RTS/M-RTS packet collision at a given time slot. Note that the collision probability will merely be related to the total number of nodes N as was derived in [43]. As shown in Fig. 6.8, when the boundary limit is less than 30 meters, the throughput performance will be the same for all the schemes except for the proposed ART-DA algorithm owing to the reason that the ART-DA scheme is primarily designed to alleviate the receiver blocking problem in multi-hop ad-hoc networks. The ART-DA protocol will result in unnecessarily excessive number of selected receivers M_i with the occurrence of failed transmission of M-RTS packets such as to deteriorate the throughput performance. Therefore, compared to the other algorithms, it can be observed that the conventional IEEE 802.11a DCF protocol can provide feasible throughput performance in the single hop ad-hoc networks. As the boundary limit B is increased, the effect of hidden nodes becomes significant to influence the on-going transmissions in the multi-hop networks. The effectiveness of the proposed ART-DA scheme is revealed such as to provide the highest throughput performance compared

to the other algorithms. Noted that the throughput performance for all the schemes is increased alone with the boundary limit since the neighbor size per node is decreased which can provide higher chance for different transmission pairs to conduct data delivery in the network.

Furthermore, it is worthwhile to evaluate the performance of proposed protocols with mobility of network nodes. The random way-point mobility (RWM) model is adopted to simulate the movement of all the nodes in the multi-hop ad-hoc network. In the RWM model, a mobile node begins by staying at a position for a random period of time called the pause time, which is determined based on a uniform distribution between $[1, t_p]$ in the unit of μs where t_p denotes the maximum pause time. After the pause time has expired, the node starts to move towards the next position which is located in the simulation area and the moving velocity is uniformly selected from $[1, V_m]$, where V_m indicates the maximum velocity of mobile node. Fig. 6.9 illustrates the throughput performance versus different maximum velocities in the left plot; while the throughput performance versus pause time is shown in the right plot. The proposed ART-DA protocol is compared to both the eMAC and the IEEE 802.11a DCF protocols. Note that the total number of node is selected as $N = 60$, the information payload size is $L = 3000$ bytes, and the boundary limit $B = 180$ meters as shown in Table 2.

It can be observed from Fig. 6.9(a) that the throughput decreases sharply after the network nodes are moving since it becomes difficult for each source node to acquire its corresponding receiver for data transmission. Afterwards, the throughput will be maintained at the same level as the maximum velocity of mobile node has been enlarged. The major reason is that most of the network connections can still be maintained in one transmission time since the velocity of each node is not large enough such that the nodes in each transmission pair will not escape from each other in such short time period.

It is intuitive to observe in each scheme that smaller pause time, i.e. $t_p = 5$ milliseconds, will result in reduced system throughput compared to that with $t_p = 2$ seconds. On the other hand, similar performance can be seen from Fig. 6.9(b) under reasonable pause time for all three schemes. The major difference is that the system throughput will be enlarged as the pause time is increased from 1 to 100 seconds, which implies that the mobile nodes will behave more stationary in the network topology. It can be observed from both plots that the proposed ART-DA protocol can outperform the other two existing schemes under various circumstances. The benefits of adopting the proposed ART protocols can therefore be observed.
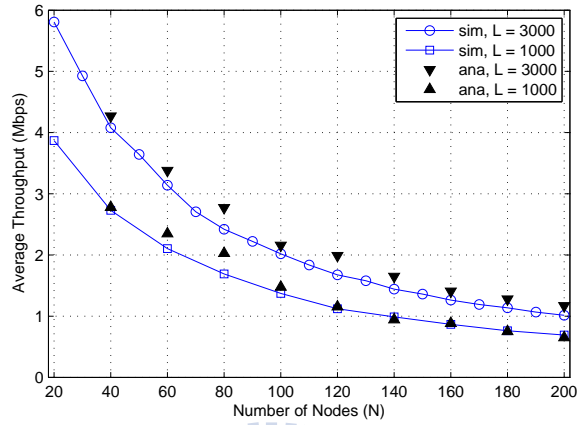
(a)
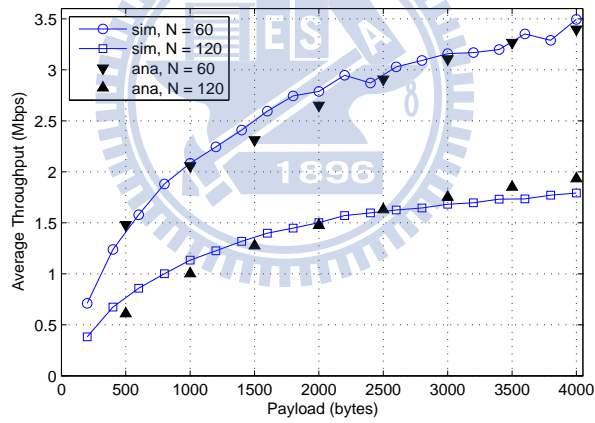
(b)

Figure 6.1: Performance validation for ART protocol with $M = 2$: average throughput versus number of nodes (top plot) and payload size (bottom plot).
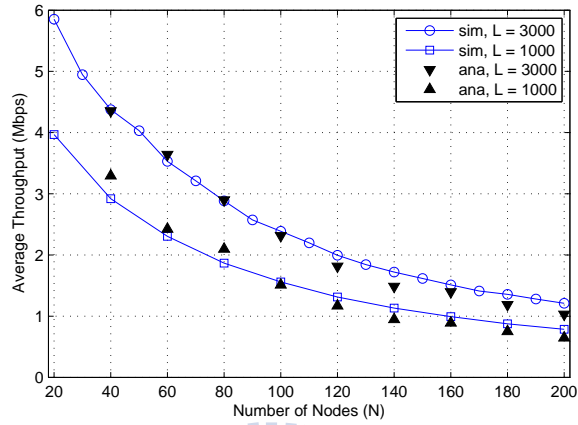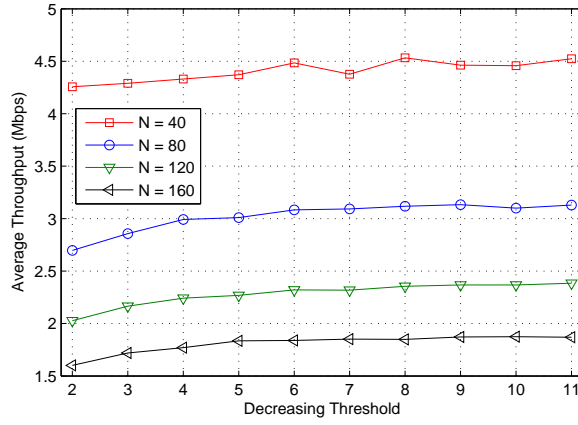
(a)
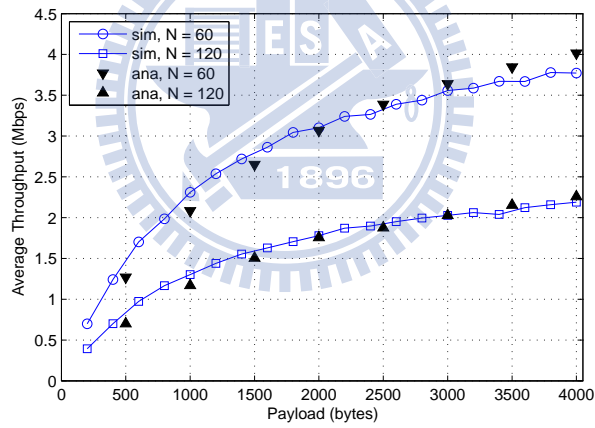
(b)

Figure 6.2: Performance validation for ART protocol with $M = 4$: average throughput versus number of nodes (top plot) and payload size (bottom plot).
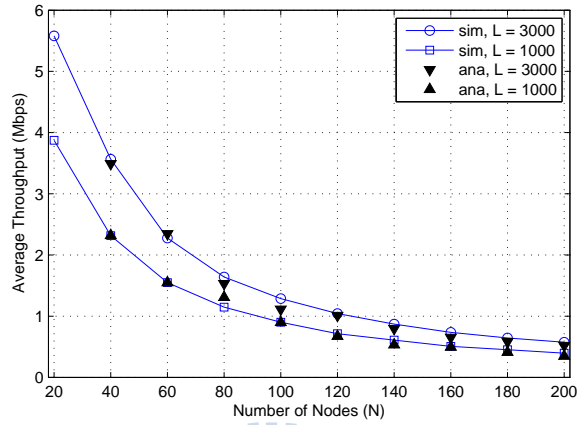
(a)
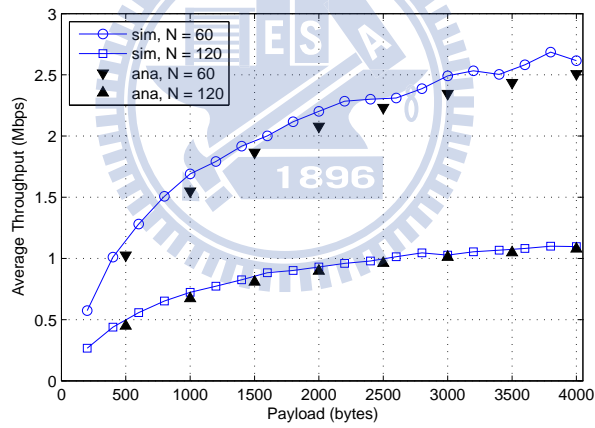
(b)

Figure 6.3: Performance validation for IEEE 802.11a DCF protocol: average throughput versus number of nodes (top plot) and payload size (bottom plot).

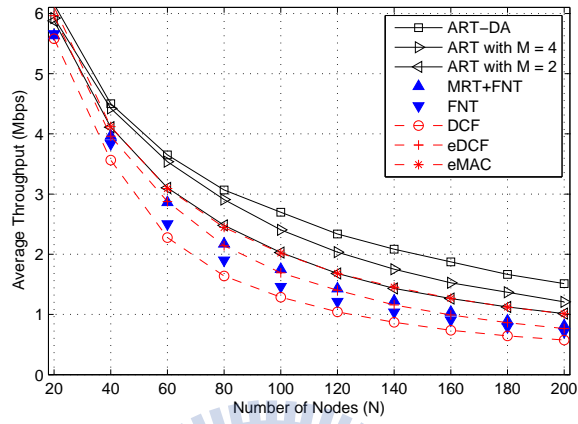Figure 6.4: Sensitivity analysis: average system throughput versus decreasing threshold Th_d.
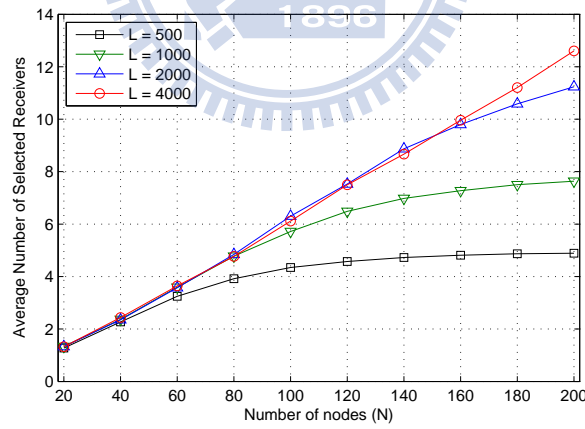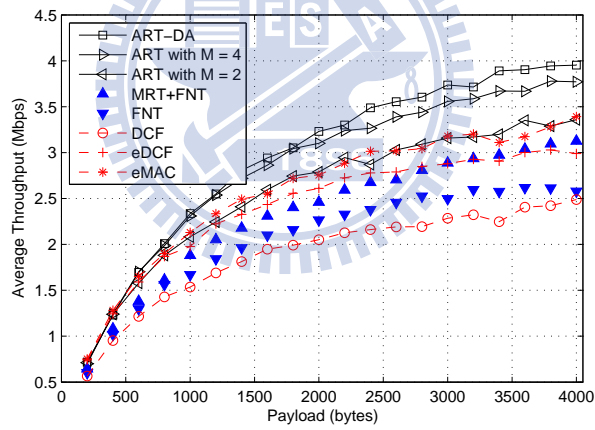

Figure 6.5: Average number of selected receivers M_i versus number of total nodes N.

(a)

(b)

Figure 6.6: Performance comparison: average throughput versus number of nodes (top plot) and payload size (bottom plot).
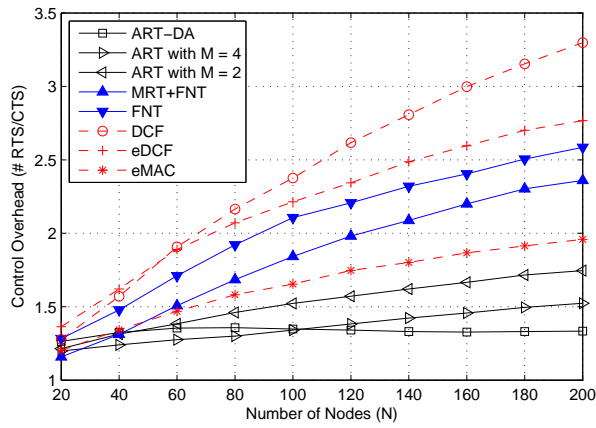
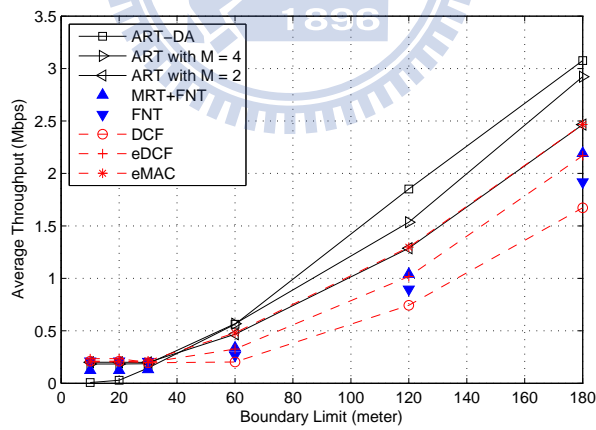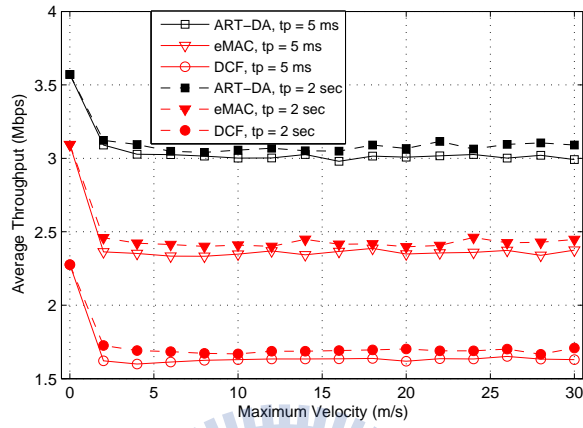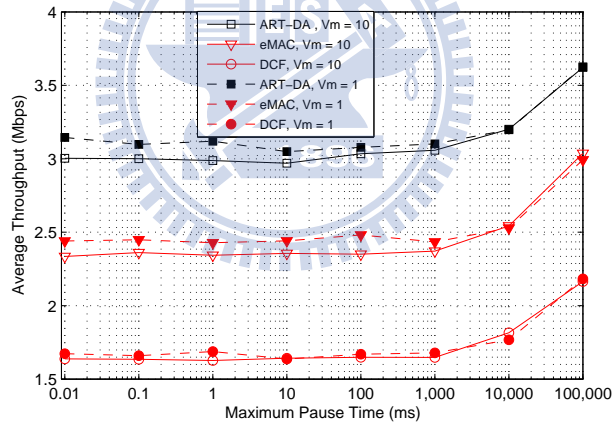Figure 6.7: Performance comparison: control overhead versus number of nodes.

Figure 6.8: Performance comparison: average throughput versus boundary limit B.

53

Figure 6.9: Performance comparison: average throughput versus maximum velocity (m/s) (top plot) and maximum pause time (ms) (bottom plot).

Chapter 7

Conclusion

In this thesis, both the multiple receiver transmission (MRT) and the fast NAV truncation (FNT) mechanisms are proposed in order to alleviate the receiver blocking problem in the multi-hop ad-hoc networks. The adaptive receiver transmission (ART) scheme is proposed to further improve the throughput performance with dynamic adjustment on the number of selected receivers. Analytical model is derived for the proposed ART scheme and is validated via simulations. It is shown in the simulation results that the proposed ART scheme can effectively alleviate the receiver blocking problem, which consequently enhances the network throughput for wireless multi-hop ad-hoc networks.

Bibliography

[1] C.S. Murthy and B.S. Mano, *Ad Hoc Wireless Networks: Architectures and Protocols*. Prentice Hall, 2004.

[2] F.A. Tobagi and L. Kleinrock, "Packet switching in radio channels:Part II-the hidden terminal problem in carrier sense multiple-access modes and the busy-tone solution," *IEEE Trans. Commun.*, vol. COM-23, no. 12, pp. 1417–1433, 1975.

[3] P. Karn, "MACA - A new channel access method for packet radio," in *Proc. ARRL/CRRL Amateur Radio 9th Computer Networking Conf.*, Sep. 1990, pp. 134–140.

[4] V. Bharghavan, A. Demers, S. Shenker, and L. Zhang, "MACAW: A media access protocol for wireless LAN's," in *Proc. ACM SIGCOMM'94*, Oct. 1994, pp. 212–225.

[5] C.L. Fullmer and J.J. Garcia-Luna-Aceves, "Floor Acquisition Multiple Access (FAMA) for Packet-Radio Networks," in *Proc. ACM SIGCOMM'95*, Oct. 1995, pp. 262–273.

[6] ——, "Solutions to hidden terminal problems in wireless networks," in *Proc. ACM SIGCOMM'97*, Oct. 1997, pp. 39–49.

[7] IEEE 802.11 WG, *IEEE Std 802.11a-1999 (R2003): Part 11: Wireless LAN Medium Access Control (MAC) and Physical Layer (PHY) specifications: High-speed Physical Layer in the 5 GHz Band*, IEEE Standards Association Std., 2003.

[8] IEEE 802.11 WG, *IEEE Std 802.11b-1999 (R2003): Part 11: Wireless LAN Medium Access Control (MAC) and Physical Layer (PHY) specifications: Higher-Speed Physical Layer Extension in the 2.4 GHz Band*, IEEE Standards Association Std., 2003.

[9] IEEE 802.11 WG, *IEEE Std 802.11g-2003: Part 11: Wireless LAN Medium Access Control (MAC) and Physical Layer (PHY) specifications: Amendment 4: Further Higher Data Rate Extension in the 2.4 GHz Band*, IEEE Standards Association Std., 2003.

[10] IEEE 802.11 WG, *IEEE P802.11n/D3.00: Part 11: Wireless LAN Medium Access Control (MAC) and Physical Layer (PHY) specifications: Amendment 4: Enhancements for Higher Throughput*, IEEE Standards Association Std., Sept. 2007.

[11] S. Xu and T. Saadawi, "Does the IEEE 802.11 MAC protocol work well in multihop wireless ad hoc networks?" *IEEE Commun. Mag.*, vol. 39, no. 6, pp. 130–137, Jun. 2001.

[12] K. Xu, M. Gerla, and S. Bae, "How Effective is the IEEE 802.11 RTS/CTS Handshake in AdHoc Networks?" in *Proc. IEEE GIOBECOM*, Nov. 2002, pp. 17–21.

[13] A. Swaminathan, D.L. Noneaker, and H.B. Russell, "The Receiver Blocking Problem in a DS Mobile Ad Hoc Network with Directional Antennas," in *Proc. IEEE MILCOM*, Oct. 2004, pp. 920–926.

[14] H. Zhai, J. Wang, Y. Fang, and D. Wu, "A dual-channel MAC protocol for mobile ad hoc networks," in *Proc. IEEE GLOBECOM Workshops*, Nov. 2004, pp. 27–32.

[15] H. Zhai, J. Wang, and Y. Fang, "DUCHA: A New Dual-Channel MAC Protocol for Multihop Ad Hoc Networks," *IEEE Trans. Wireless Commun.*, vol. 5, no. 11, pp. 3224–3233, Nov. 2006.

[16] B. Zhou, A. Marshall, and T.H. Lee, "The Non-Responsive Receiver Problem in Mobile Ad-Hoc Networks," *IEEE Commun. Lett.*, vol. 9, no. 11, pp. 973–975, Nov. 2005.

[17] S.R Ye, Y.C. Wang, and Y.C. Tseng, "A jamming-based MAC protocol for wireless multihop ad hoc networks," in *Proc. IEEE VTC-Fall*, Oct. 2003, pp. 1396–1400.

[18] Y. Gu, L. Shen, and X. Qiu, "A dual-channel MAC protocol for multi-hop ad hoc networks," in *Proc. IEEE ICCCAS*, May 2005, pp. 308–313.

[19] K. Ghaboosi, M. Latva-aho, and Y. Xiao, "Receiver blocking problem in mobile ad hoc networks: Challenges & solutions," in *Proc. IEEE WD'08*, Nov. 2008, pp. 1–5.

[20] K. Ghaboosi, M. Latva-aho, Y. Xiao, and Q. Zhang, "Unreachability problem in mobile ad hoc networks: A medium access control perspective," in *Proc. IEEE PIMRC*, Sept. 2009, pp. 2576–2580.

[21] D. Tse and P. Viswanath, *Fundamentals of Wireless Communication*. Cambridge University Press, 2005.

[22] J. Deng and Z.J. Haas, "Dual busy tone multiple access (DBTMA): a new medium access control scheme for packet radio networks," in *Proc. IEEE ICUPC'98*, Oct. 1998, pp. 973–977.

[23] Z.J. Haas and J. Deng, "Dual busy tone multiple access (DBTMA)- performance evaluation," in *Proc. IEEE VTC'49*, Jul. 1999, pp. 314–319.

[24] ——, "Dual busy tone multiple access (DBTMA)- a multiple access control scheme for ad hoc networks," *IEEE Trans. Commun.*, vol. 50, no. 6, pp. 975–985, Jun. 2002.

[25] B. Ji, "Asynchronous busy-tone multiple access with acknowledgement (ABTMA/ACK) for ad hoc wireless networks," in *Proc. IEEE GLOBECOM*, Dec. 2005, pp. 3643–3647.

[26] W. Yuan, G. Zhu, G. Liu, D. Wu, and M. Chen, "A New MAC Protocol of Ad Hoc Networks," in *Proc. IEEE VTC-Fall*, Sept. 2007, pp. 1618–1622.

[27] P. Wang and W. Zhuang, "An Improved Busy-Tone Solution for Collision Avoidance in Wireless Ad Hoc Networks," in *Proc. IEEE ICC*, Jun. 2006, pp. 3802–3807.

[28] H. Zhai and Y. Fang, "A Solution to Hidden Terminal Problem Over a Single Channel in Wireless AD HOC Networks," in *Proc. IEEE MILCOM*, Oct. 2006, pp. 1–7.

[29] K. Ghaboosi, M. Latva-aho, Y. Xiao, and Q. Zhang, "eMAC - A Medium Access Control Protocol for the Next Generation Ad Hoc Networks," *IEEE Trans. Veh. Technol.*, vol. 58, no. 8, pp. 4476–4490, Oct. 2009.

[30] K. Ghaboosi and B.H. Khalaj, "AMACA - a new multiple access collision avoidance scheme for wireless LANS," in *Proc. IEEE PIMRC*, Sept. 2004, pp. 1932–1936.

[31] D. Lihong and J. Yan'an, "A Novel MAC Protocol for Hidden Receiver Problem in Ad Hoc Networks," in *Proc. IEEE ICAL*, Aug. 2007, pp. 2345–2348.

[32] A. Chayabejara, S.M.S. Zabir, and N. Shiratori, "An enhancement of the IEEE 802.11 MAC for multihop ad hoc networks," in *Proc. IEEE VTC-Fall*, Oct. 2003, pp. 3020–3024.

[33] L.B. Jiang and S.C. Liew, "Improving Throughput and Fairness by Reducing Exposed and Hidden Nodes in 802.11 Networks," *IEEE Trans. Mobile Comput.*, vol. 7, no. 1, pp. 34–49, Jan. 2008.

[34] ——, "Hidden-Node Removal and Its Application in Cellular WiFi Networks," *IEEE Trans. Veh. Technol.*, vol. 56, no. 5, pp. 2641–2654, Sept. 2007.

[35] Y. Zhou and S.M. Nettles, "Balancing the hidden and exposed node problems with power control in CSMA/CA-based wireless networks," in *Proc. IEEE WCNC*, Mar. 2005, pp. 683–688.

[36] K. Liu and X. Xing, "A Multichannel Reservation Multiple Access Protocol for Mobile Ad Hoc Networks," in *Proc. IEEE ICC*, May 2008, pp. 3176–3180.

[37] T. Luo, M. Motani, and V. Srinivasan, "CAM-MAC: A Cooperative Asynchronous Multi-Channel MAC Protocol for Ad Hoc Networks," in *Proc. IEEE BroadNets*, Oct. 2006, pp. 1–10.

[38] J. Chen and Y.D. Chen, "AMNP: ad hoc multichannel negotiation protocol for multihop mobile wireless networks," in *Proc. IEEE ICC*, Jun. 2004, pp. 3607–3612.

[39] J. Chen, S.T. Sheu, and C.A. Yang, "A new multichannel access protocol for IEEE 802.11 ad hoc wireless LANs," in *Proc. IEEE PIMRC*, Sept. 2003, pp. 2291–2296.

[40] S.C. Lo and C.W. Tseng, "A Novel Multi-Channel MAC Protocol for Wireless Ad Hoc Networks," in *Proc. IEEE VTC-Spring*, Apr. 2007, pp. 46–50.

[41] K. Liu, T. Wong, J. Li, L. Bu, and J. Han, "A reservation-based multiple access protocol with collision avoidance for wireless multihop ad hoc networks," in *Proc. IEEE ICC*, May 2003, pp. 1119–1123.

[42] E. Shim, S. Baek, J. Kim, and D. Kim, "Multi-Channel Multi-Interface MAC Protocol in Wireless Ad Hoc Networks," in *Proc. IEEE ICC*, May 2008, pp. 2448–2453.

[43] G. Bianchi, "Performance Analysis of the IEEE 802.11 Distributed Coordination Function," *IEEE J. Sel. Areas Commun.*, vol. 18, no. 3, pp. 535–547, Mar. 2000.

[44] F. Alizadeh-Shabdiz and S. Subramaniam, "Analytical models for single-hop and multi-hop ad hoc networks," in *Proc. IEEE BroadNets*, Oct. 2004, pp. 449–458.

[45] ——, "MAC layer performance analysis of multi-hop ad hoc networks," in *Proc. IEEE GLOBECOM*, Nov. 2004, pp. 2781–2785.

[46] P. Li and Y. Fang, "Saturation throughput of IEEE 802.11 DCF in multi-hop ad hoc networks," in *Proc. IEEE MILCOM*, Nov. 2008, pp. 1–7.

[47] T.C. Hou, L.F. Tsao, and H.C. Liu, "Analyzing the throughput of IEEE 802.11 DCF scheme with hidden nodes," in *Proc. IEEE VTC-Fall*, Oct. 2003, pp. 2870–2874.

[48] A.A. Abdullah, F. Gebali, and L. Cai, "Modeling the Throughput and Delay in Wireless Multihop Ad Hoc Networks," in *Proc. IEEE GLOBECOM*, Nov. 2009, pp. 1–6.

[49] Y. Wang and J.J. Garcia-Luna-Aceves, "Collision avoidance in multi-hop ad hoc networks," in *Proc. IEEE MASCOT*, 2002, pp. 145–154.

[50] B.J. Kwak, N.O. Song, and L.E. Miller, "Performance Analysis of Exponential Back-off," *IEEE/ACM Trans. Netw.*, vol. 13, no. 2, pp. 343–355, Apr. 2005.